TECHNISCHE
UNIVERSITÄT
WIEN
Vienna University of Technology

Vienna University of Technology

Institute of Applied Physics

Surface Science

Bachelors Thesis

Title

Author:
Martin Kronberger

Supervisor:

January 1, 2025

Declaration of Authorship

Martin Kronberger

I hereby declare that I have written this thesis independently and that I have fully acknowledged all the sources and aids used. Furthermore, I confirm that I have marked as borrowed any parts of this work (including tables, maps, and figures) that are taken from other works or from the internet, either verbatim or in spirit, giving explicit reference to the source.

I further declare that large language models were used solely to assist with formatting, providing code snippets, and helping to resolve minor technical issues. These models did not contribute to the research content, analyses, interpretations, conclusions, or any intellectual substance of this thesis.

Martin Kronberger
Vienna, 1 January 2025

Acknowledgements

Danksagung

Abstract

Kurzfassung

Contents

Introduction

Catalysis is an inseparable part of modern society, relying on the chemical industry, solutions in ecology, or effective energy storage. Therefore, the development of superior catalysts has been in the scope of surface science for many years.

One of the approaches is the preparation and investigation of model catalysts in the form of single crystal support with well-defined active sites. The use of inexpensive support materials and the reduction of deposited noble metals significantly increase the effectiveness and selectivity of model catalysts. Such a catalyst configuration also enables a better understanding of physical processes happening on its surface.

However, their preparation and investigation require ultra-high vacuum (UHV) to preserve adequate inertness of the surrounding environment. Therefore, the laboratory pressure conditions usually do not reflect the real industrial setup. To bridge this pressure gap, the microreactor (high-pressure cell) located in the UHV chamber, enabling sample exposure to elevated gas pressure and temperature, is under development.

There are several similar devices in use, however, their microscopic flow description is often trivialized. And particularly flow conditions at the reactive surface have a significant influence on the reactant and product transportation. Omitting these factors can then result in a misleading read of the catalytic activity.

The main scientific task is to get an uncomplicated and reliable overview of the macroscopic gas flow properties inside the high-pressure cell located in the UHV chamber. The appropriate gas flow theory is presented initially and later applied to certain geometry and required conditions. The main attention was paid to selected, most-critical locations in the micro reactor. The obtained results, respectively the formulated approach to calculate gas properties, are essential for ongoing microscopic flow investigation, and can be easily applied on adjusted geometry of high-pressure cells.

1 Scope and objectives

The aim of this thesis is to develop a straightforward analytical framework that predicts flow behavior and estimates state variables at key positions within a micro-reactor assembly. These estimates will later serve as initial conditions for more detailed numerical simulations. Figure 1 illustrates the reactor configuration, where reactants are mixed in the reservoir, pass through the inlet and reaction volume, and finally exit into the vacuum through the outlet—with a portion of the gas leaking at the reactor's sealing interface.

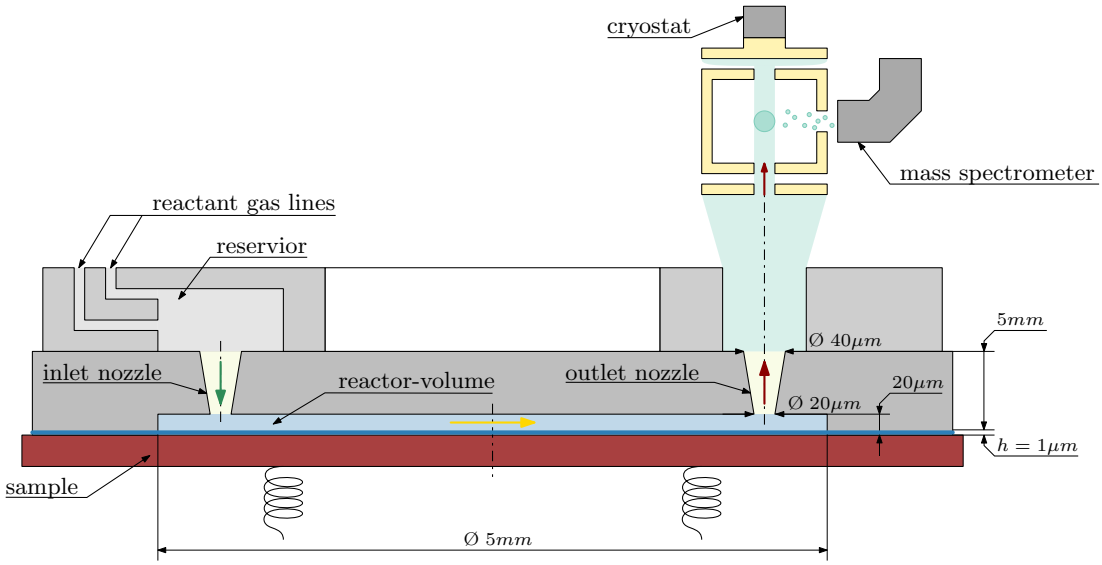

Figure 1: Schematics of the micro-reactor assembly [1]: The reactants are mixed in the reservoir, pass progressively through the inlet (green arrow), reaction volume (yellow arrow), and exhaust into the vacuum through the outlet (red arrow). The exhaust gas composition is analyzed via quadrupole mass spectroscopy. The part of the gas in the reaction volume leaks through the space between the sample and the sealing surface of the reactor (blue arrow).

In the sections that follow, we address four main objectives: identifying the dominant flow regime, quantifying the impact of leakage, characterizing the gas state in the vicinity of the sample, and predicting the velocity distribution at the outlet. To achieve these goals, the analysis relies on established concepts such as the Knudsen and Reynolds numbers, along with one-dimensional isentropic flow theory. This foundation, which is detailed in the subsequent chapter on foundational principles, not only clarifies the interaction between the reactor's geometry and gas dynamics but also lays the groundwork for future numerical simulations and experimental studies.

1.1 Type of Flow

The type of flow has major implications on which mathematical formulations and simulations are applicable, as well as the way the gas particles interact with each other and the walls of the assembly. The main focus here is the Knudsen number and the idealized flow regimes connected to it. With the main goal being to assess the most likely flow regime governing the inside of the assembly and therefore determine the equations applicable to calculate the state variables at different points in the system and the throughput of the system as a whole.

In preparation for numerical simulations it is also important to find a way to calculate Knudsen numbers and other flow parameters using given datasets of state variables

without having to rely on flow regime specific methods. This will help to analyze transient regimes, encountered when the gas expands into the vacuum, using one generally applicable method.

1.2 Impact of the leak

As described in the leading section there will be some leakage expected at the boundary between the reactor casing and the sample holder. This leak will inevitably lead to some mass-flow and therefore some pressure drop ΔP_L inside the reactor. This can lead to major changes to the steady state of the system, therefore influencing the velocity distribution at the outlet. In summary the goal is finding the pressure drop ΔP_L caused by the leak and the effective mass flow $\dot{m}_L$ through it and use them to predict probable behaviors.

1.3 Behavior of the gas around the sample

Knowing more about the state the gas is in close to the sample is very helpful. These can be used to estimate values for diffusion rates to and from the surface, boundary layer thickness, and mean velocities and momentum of particles reaching the reactive surface. Important metrics are the velocity, pressure and temperature of the gas and the type of flow.

1.4 Velocity distribution at the outlet

After the gas leaves the outlet nozzle, it expands into a vacuum chamber where the gas atoms are ionized by an electron beam and picked up by the mass-spec, to measure the ratio of different products. This won't be the case for all atoms, since for an atom to be ionized it has to cross the electron beam, which is localized in space. The remaining gas has to be pumped out and doesn't contribute to the ratio measured by the mass-spec. Therefore, it is important to approximate, how much of the gas leaving the outlet actually is able to reach the region of influence of the electron beam and will contribute to the measurement of the mass-spec. To answer this the velocity distribution of the expansion after the gas is fully rarefied is needed. This distribution can then essentially be treated as a source like surface, with no interaction between gas particles, and can therefore be directly correlated to the amount of atoms reaching the sphere of influence of the electron beam.
Knowing what determines the distribution of the outlet can also help identify changes to be made to the geometry or the reservoir conditions to increase the amount of atoms reaching the mass-spec.

2 Foundational Principles

When dealing with advanced fluid dynamical systems, before being able to formulate models to solve them, they have to be categorized. This is usually done by determining dimensionless numbers which values ought to describe more the behavior of the gas and its interaction with its surrounding. Essentially the values of these dimensionless numbers give a clue on which formulations are applicable and if additional boundary conditions or considerations have to be taken into account. This first chapter will go into the details of how to calculate some of the most important dimensionless numbers and give insight on what the values of them imply.

2.1 Characteristic Length

The characteristic length essentially serves the purpose of scaling physical systems. In dimensional analysis the goal is to find dimensionless quantities which describe the behavior of the system. These quantities are usually dependent on some characteristic scale, in our case the length scale, which describes the geometry of the model abstractly. For internal flows the characteristic length is defined as:

$$L_c = \frac{4A}{P_w} \quad \text{with} \quad P_w = \sum_{i=0}^{\infty} l_i \tag{2.1}$$

Where A is the cross-sectional area and P_w is the wetted perimeter, which is defined as the sum over the lengths of all surfaces in direct contact with the fluid. For gaseous fluids the whole perimeter of the cross-section must be considered, therefore the wetted perimeter reduces to the perimeter of the cross-section. The following section provides the characteristic length formulas for common duct shapes. [2]

circular duct

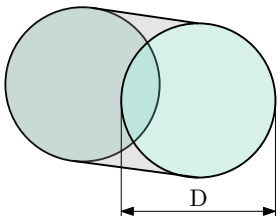

$P_{w_\circ} = \pi D \quad \rightarrow \quad L_{c_\circ} = D$

rectangular duct

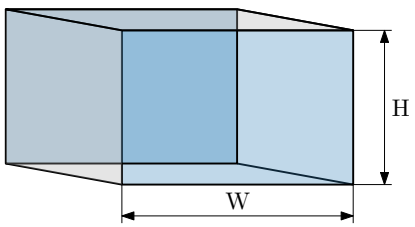

$P_{w_\square} = 2H + W \quad \rightarrow \quad L_{c_\square} = \frac{2HW}{H+W}$

If the height H of a rectangular duct is very small compared to its width W, it is more convenient to view it as an asymptotic case where the width approaches infinity ($W \rightarrow \infty$).

two parallel plates

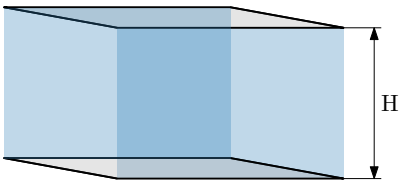

$\lim_{W\to\infty} L_{c_\square} = \lim_{W\to\infty} \frac{2HW}{H+W} = 2H$

2.2 Turbulence and the Reynolds number

To distinguish between different kinds of flow behaviors in fluid mechanics a dimensionless quantity is introduced, which describes the ratio between inertial forces and viscous forces inside a fluid. This quantity is called the Reynolds number and is defined as:

$$Re = \frac{\rho u L_c}{\mu} = \frac{uL}{\nu} \tag{2.2}$$

Where ρ is the fluid density, u is the flow speed, L is a characteristic length (such as pipe diameter), μ is the dynamic viscosity, and ν is the kinematic viscosity. These flow behaviors can be sorted into three categories depending on the value of the Reynolds number:

- Laminar flow $Re < 2000$: where fluid moves in smooth layers, with minimal mixing between those layers.
- Transitional flow $2000 \geq Re \geq 4000$: marks the transition between the main regimes.
- Turbulent flow $Re > 4000$: where the fluid moves chaotic and mixes irregularly due to formation of eddies.

[3, 4]

2.3 Rarefaction and the Knudsen number

In fluid dynamics a flow can be categorized by its particle interaction using the Knudsen number, which represents the ratio between the mean-free-path λ of the gas and the characteristic length L_c of the flow geometry.

$$Kn = \frac{\lambda}{L_c} \tag{2.3}$$

Molecular regime ($Kn \geq 10$)

In this regime, the mean free path is much larger than the dimensions of boundaries. This leads to particle interactions themselves becoming negligible in comparison to the interaction of particles with the boundary.

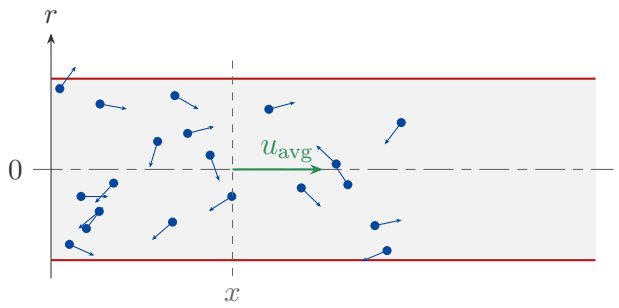

Figure 2: Schematic of the velocity distribution at a cross-section in a circular duct under molecular flow conditions. The red lines denote the duct boundaries, the green arrow and line represent the mean velocity at position x, blue dots and arrows represent individual particles and their velocity.

Transition regime ($0.1 \leq Kn \leq 10$)

This regime is a middle ground between continuum and fully molecular flow. Neither the continuum assumptions of fluid dynamics nor the free molecular flow assumptions hold completely. The interactions between the gas molecules and the boundaries are significant, and the flow characteristics may vary widely.

Slip regime ($0.001 \leq Kn \leq 0.1$)

For increasing Knudsen numbers the mean free path becomes comparable to the characteristic length scale of the system. In this regime, the assumptions for continuum flow still hold, but there are deviations, especially near the boundaries. While continuum mechanics assumes no-slip conditions on the boundary, in this regime, slip on the boundary must be factored in.

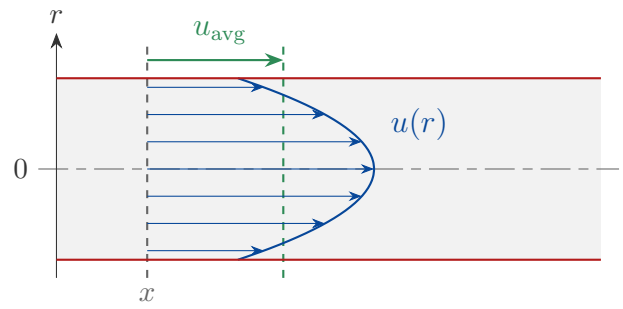

Figure 3: Schematic of the velocity distribution at a cross-section in a circular duct under slip flow conditions. The red lines indicate the duct boundaries, the green arrow and line denote the mean velocity at position x, and the blue function with arrows shows the velocity profile modified by slip effects at the walls. [3]

Continuum regime ($Kn \leq 0.001$)

In this regime, the interactions of particles in the medium are much more frequent than the interactions of particles with the boundaries of the duct. This makes it possible to describe the fluid itself as a continuous medium with the assumption of non-slip boundary conditions. The Navier-Stokes equations govern the calculations in this regime.

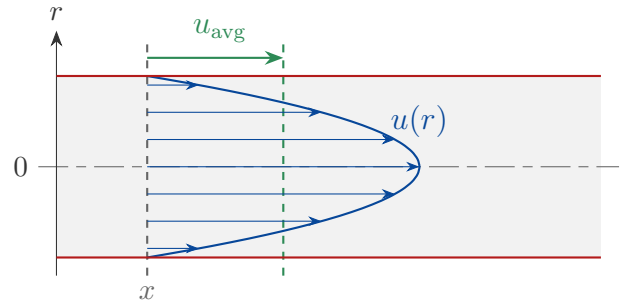

Figure 4: Schematic of the velocity distribution at a cross-section in a circular duct under continuum flow conditions. The red lines mark the duct boundaries, the green arrow and line indicate the mean velocity at position x, and the blue curve with arrows represents the classical velocity profile typical of fully developed laminar flow. [3]

In this work the continuum formulations will be used exclusively, with the reasons more clearly described in chapter 3.2. [5, 6, 7, 2]

2.4 Dimension of the flow

The dimension describes the number of positional parameters needed to yield an exact solution for a given vector field $V(\vec{x})$, so equals essentially $n = \dim(\vec{x})$. The flow through a constant area duct is usually described as a one-dimensional flow field only depending on the position x along the length of the duct. In the case of variable area ducts the flow will be three-dimensional and has to be calculated using all spatial coordinates. But assuming only a slight change in area along the length of the duct the flow can be approximated using a one-dimensional flow field with enough precision. This is called quasi one dimensional flow. [4]

2.5 Isentropic one-dimensional flow

Isentropic varying-area flow is one of the most idealized models to describe the behavior of gases flowing through a confined space. The following assumptions are made:

- steady, one-dimensional flow
- adiabatic: $\delta q = 0, ds_e = 0$
- no shaft work: $\delta w_s = 0$
- negligible change in potential energy: dz = 0
- reversible: $ds_i = 0$

Being reversible as well as adiabatic, the flow is therefore isentropic. The gas is still considered perfect and follows the perfect gas law, as it is crucial in the derivation for the following relations which are the foundation for solving isentropic one-dimensional gas flows. Flow velocity for continuum flows is usually encoded into the Mach number, which is defined as the ratio between the local velocity u and the local speed of sound a.

$$Ma = \frac{u}{a} \tag{2.4}$$

It is a very important metric when analyzing isentropic flow, since state variables are uniquely defined through the mach number at the corresponding location, as long as either the stagnation, or critical conditions of the flow are known. For isentropic flow one-dimensional flow it can be directly linked to the geometry of the duct and can be calculated by defining a state in the system where Mach number is equal to 1, the so-called throat. Then its area is related to the Mach number by following non-linear equation:

$$\frac{A}{A^*} = \frac{1}{Ma}\left[\frac{2}{\gamma+1}\left(1+\frac{\gamma-1}{2}M^2\right)\right]^{\frac{\gamma+1}{2(\gamma-1)}} \tag{2.5}$$

Where A represents the area of the duct at some location, A^* the area of the throat, Ma the Mach number at the given location and γ the ratio of heats. One of the most important ideas in isentropic flow are the stagnation/total conditions, which represent the state of a moving gas when fully decelerating it isentropicaly ($Ma = 0$). They exist for the fundamental state variables of the gas notated as ($P_0,\ T_0,\ \rho_0$) and represent conserved quantities when dealing with isentropic flow. This stagnation state does not have to exist in the system, but can also be derived if velocity and state variables at some point in the system are known. Total conditions represent the highest values of any state variable reachable in the system, while still being insentropic. Therefore, changes of state variables are usually represented in relation to the total conditions of

the corresponding state variables, and depend only on the ratio of heats of the gas γ and the Mach number Ma.

$$\frac{T}{T_0} = \left(1 + \frac{\gamma - 1}{2} Ma^2\right)^{-1} \tag{2.6}$$

$$\frac{p}{p_0} = \left(1 + \frac{\gamma - 1}{2} Ma^2\right)^{-\frac{\gamma}{\gamma - 1}} \tag{2.7}$$

$$\frac{\rho}{\rho_0} = \left(1 + \frac{\gamma - 1}{2} Ma^2\right)^{-\frac{1}{\gamma - 1}} \tag{2.8}$$

Low subsonic regime ($Ma < 0.3$) For low Mach numbers, compressibility effects of a gas can be neglected, and the gas can be treated as an incompressible fluid. In figures locations where the flow is probable to have very low Mach-numbers will be indicated by a yellow arrow (as seen in figure 1).

Subsonic regime ($0.3 < Ma < 1.0$) Inside system of variable area ducts the gas flow generally stays subsonic. Once sonic speed is reached in a converging duct, the behavior reverses, and the velocity decreases, limiting the flow to subsonic or sonic speeds within converging ducts. In figures, locations where the flow can be assumed subsonic will be indicated by a green arrow (as seen in figure 1).

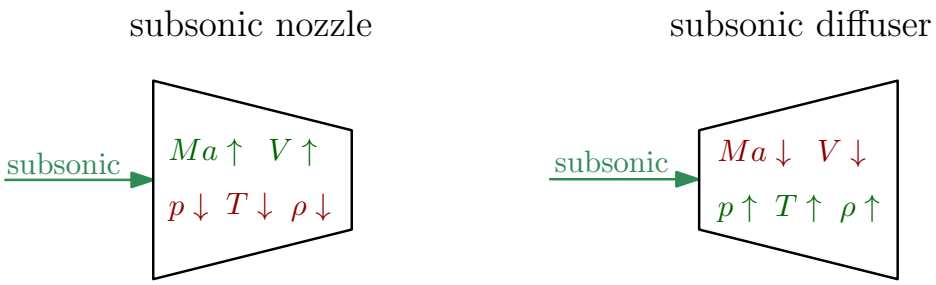

Figure 5: Schematic illustrating changes in state variables for subsonic flow in a converging nozzle (left) and a diverging diffuser (right). A green arrow indicates subsonic flow entering each device. In the nozzle, Mach number and velocity increase while pressure, temperature, and density decrease. Conversely, in the diffuser, Mach number and velocity decrease, and pressure, temperature, and density rise. [3]

Sonic regime ($Ma = 1$) Sonic flow occurs at the exit of a converging duct, if the pressure ratio between two reservoirs becomes smaller than the following critical ratio. Which is called chocked flow and constitutes the maximum mass-flow for given stagnation conditions. This ratio is defined as:

$$\frac{P^*}{P_0} = \left(\frac{2}{\gamma + 1}\right)^{\frac{\gamma}{\gamma - 1}} \tag{2.9}$$

Where P_0 is the stagnation condition, P^* the critical back-pressure and γ the specific heat ratio. The ratio is derived from the isentropic flow relation (2.6) and can be expressed for any state variable which are explicitly stated in the formulary.

Supersonic regime ($Ma > 1$) If there are critical conditions at the end of a converging duct and a diverging duct follows. The flow continues to accelerate and reaches supersonic speeds. The location where the flow reaches critical condition is called throat

and represents the minimal diameter of the duct.
In supersonic flows, state variables change rapidly causing phenomenons like shock waves and expansion fans. Just like the previous regimes, this regime will be indicated using an arrow colored red. [8]

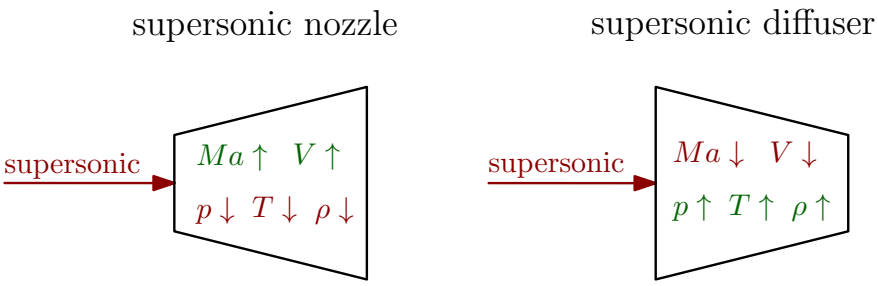

Figure 6: Schematic illustrating changes in state variables for supersonic flow in a diverging nozzle (left) and a converging diffuser (right). A red arrow indicates supersonic flow entering each device. In the nozzle, Mach number and velocity increase while pressure, temperature, and density decrease. Conversely, in the diffuser, Mach number and velocity decrease, and pressure, temperature, and density rise. [3]

Massflow Mass flow is conserved along the flow and can be calculated using following equation, which derives from the equation for mass-flow in a steady one-dimensional flow (2.10), the isentropic relations [(2.6) - (2.7)] and the ideal gas law. [9]

$$\dot{m} = A \cdot P_0 \cdot \sqrt{\frac{\gamma}{RT_0}} \cdot M \cdot \left(1 + \frac{\gamma - 1}{2} M^2\right)^{-\frac{\gamma+1}{2(\gamma-1)}} \tag{2.10}$$

Relation of dimensionless numbers in continuum flow It is possible to relate the three dimensionless numbers mentioned in the preceding chapters. Leading to following relation:

$$Kn = \frac{Ma}{Re} \sqrt{\frac{\gamma\pi}{2}} \tag{2.11}$$

Where Ma is the Mach-number, Re the Reynolds-number and Kn the Knudsen-number at some point in the flow of gas with the ratio of heat γ. [3, 10, 11]

3 Analytical work

Now that the fundamental principles used are set, this chapter focuses on answering as many questions from chapter 1. First the geometry is defined in a more rigorous way, to be able to define the characteristic lengths for every important point inside the assembly. While also defining the conditions inside the reservoir and the vacuum and how they influence the flow. Afterward, the expected flow regimes will be assumed, to confirm that the isentropic continuum flow regime is applicable. These assumptions will be confirmed by the following analytical calculations. Where first the assembly will be approximated by a variable area duct, without any leakage in the system, where one-dimensional isentropic flow formulations can be applied, and the assumptions made in the preceding chapter can be tested. Since this approximation come with a cost, mainly by ignoring the geometry and possible non-isentropic behavior in the reactor. Therefore, a short section going into behaviors in micro-channels and the problem of slip on the boundaries follows, which paves the way for a more elegant formulation, where the reactor is seen as its own reservoir with given stagnation conditions. Since a change in stagnation conditions corresponds to non-isentropic flow behavior, is trying to include those while still treating the parts isentropically in isolation. This makes it possible to include mass-flow of the leak in the reactor, whose influence on the Mach number of the inlet throat will be explored. Ending with a short argument on why using the given formulations are not applicable to solve the velocity distribution at the outlet and therefore possible numerical solutions are presented.

3.1 Geometry and flow characteristics of the components

The geometry can be explained in three simple sections: gas from a reservoir flows over the inlet into the micro-reactor where it leaves through the outlet into a vacuum. This is a stark simplification, but for a great part of this thesis, this is how we will imagine our flow path. This is because the only thing we left out is any kind of leak in the system. Those leaks will be the most influential around the reactor, since this is the only part that is not held at a constant pressure by any external part of the system.

Reservoir

It is kept at constant pressure P_0 and constant temperature T_0, out of which the density ρ can be calculated. These values will represent the stagnation or total conditions of the system, where the flow velocity is zero. The parts of the flow where stagnation conditions are assumed will be represented using a gray hue. For simplicity, it contains only one gas which is defined by its specific heat ratio γ and by its molar mass M_m. The Formulations used yield the changes in pressure, temperature and density as ratios between the local conditions and the stagnation conditions Therefore, there is no need to define stagnation conditions explicitly beforehand, since local conditions can be calculated for by multiplying chosen stagnation conditions with the calculated ratios. Therefore, only the parameters of the gas have to be defined up front, which will be defined as:

$$\gamma = 1.47\ , \qquad M_m = 28.013\ \frac{\mathrm{g}}{\mathrm{mol}}$$

representing nitrogen gas (N_2), since it is comparable to the gases planned to use in experiments.

Inlet/Outlet Nozzles

Inlet The duct connecting the inlet reservoir with the reactor will be a slightly converging duct, due to production constraints. Therefore, it will act like a Nozzle, accelerating the gas until it expands into the reactor.

Outlet With the same geometry as the inlet, but the gas flowing in opposite directions, one would suspect the outlet to act as a subsonic nozzle, which could logically be the case, since without a converging section in front it would be impossible to reach sonic velocities and therefore will choke the flow and keep them at subsonic velocities. However, it is actually possible for the flow to create a converging section by itself, which will force the flow to be sonic at the beginning of the outlet and will further accelerate into the supersonic regimes, creating a supersonic nozzle. [12]

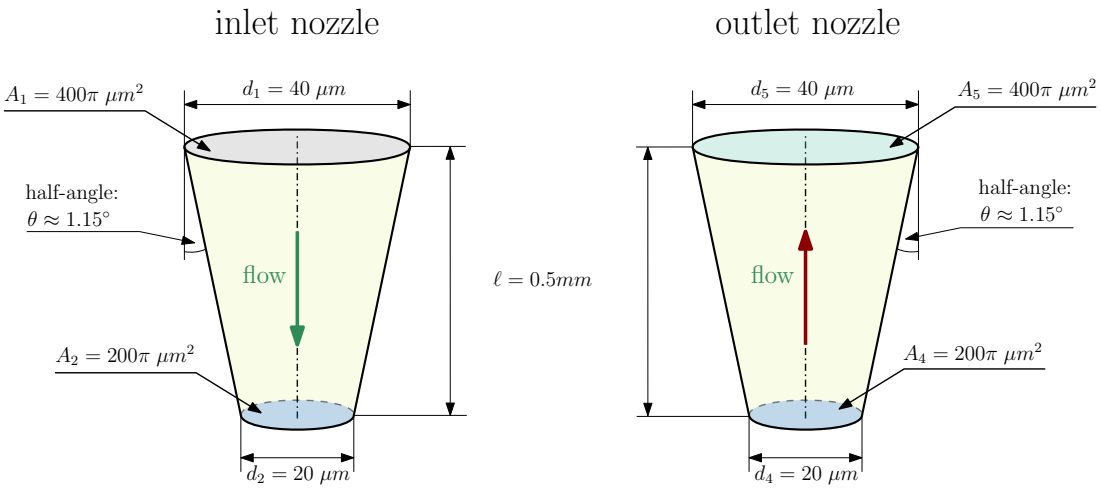

Figure 7: Schematic of the inlet and outlet nozzle assembly. Yellow-shaded regions denote domains where one-dimensional flow is assumed. Flow is indicated by colored arrows: green arrows represent subsonic flow and red arrows indicate supersonic flow. In the downstream expansion region, the flow is modeled as two-dimensionally rotationally symmetric (green-shaded). This schematic is not drawn to scale

Nozzle flow - pseudo 1D In these sections of the flow a simplification of the two-dimensional flow through a duct will be used called "quasi one-dimensional" flow. This is possible by reducing the velocity distribution present at any point along the length of a duct to its mean velocity. Therefore, reducing the velocity from a distribution $V(r)$ at every point in the duct to a scalar value V at every point of the duct. This is a general simplification which can be made when using continuum flow analysis inside of ducts with reasonable small change in cross-sectional area and is only bound by the applicability of continuum flow as described in chapter 2.4. One-dimensional flow will be represented using a yellow hue, as seen in the volume of the nozzles in figure 7. [4]

Micro-Reactor Volume

The reactor resembles a very small but broad cylinder shape which is opened at the bottom. The sample will be pressed into the opening, which will lead to some leakage out of the system.

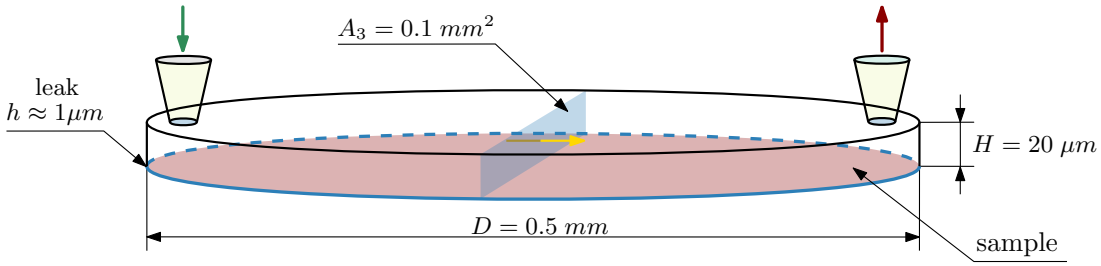

Figure 8: Schematic of the reactor geometry. The reactor volume is shown in blue to represent the region where three-dimensional flow occurs. The sample surface is indicated in red, and the leak is marked by a blue outline along the reactor perimeter. Flow characteristics are depicted by colored arrows: yellow arrows for slow-moving flow, green arrows for subsonic flow, and red arrows for supersonic flow. This diagram is not drawn to scale.

Flow through the reactor - 3D After the gas flow leaves the inlet nozzle and streams into the reactor chamber, the geometry of the assembly has no symmetry to reduce the dimension of the velocity field. Additionally, there is rapid expansion of the gas since the constraints given by the walls of the nozzle are now gone and the gas flows over a sharp corner. Therefore, the flow field has to be dependent on all spacial dimensions and essentially means the only way to get an accurate representation of the flow field the Navier-Stokes equations have to be solved. This won't be possible using only analytical tools, therefore in the following sections two simplifications of the flow through the reactor will be used. At first, assuming pseudo one-dimensional flow throughout the reactor, which is definitely wrong, since the flux area is neither expanding very slowly, nor the flow will be isentropic, due to the expansion into free space. To address this issue and still be able to use analytical tools to solve the system, in chapter 3.5 the reactor will be assumed to be a reservoir. Three-dimensional flow will be represented using a blue hue as seen in the middle of the reactor in figure 8.

Vacuum

After leaving the outlet, the gas will first expand into a small cylindrical section after which it will expand freely into the vacuum. The exact pressure left in the vacuum chamber does not influence the gas flow inside the assembly since the large pressure ratio between reactor and vacuum will force the flow to be chocked, and thus the back pressure looses its influence. Due to the sharp change in pressure and the high velocity of the gas particles the gas will transition to the molecular regime after leaving the outlet nozzle.

Free jet into vacuum - 2D Similar to the flow into the reactor, the flow out of the system into the vacuum chamber won't be reducible to pseudo one-dimensional flow anymore. But this time the fact that the outlet nozzle is radially symmetric and there is no further geometry constraining the flow after it leaves the outlet. The flow can be at least assumed to inherit the radial symmetry from the outlet nozzle, thus reducing the spacial parameters of the flow field to the distance from the nozzle and the distance from the axis of symmetry of the outlet nozzle r. Furthermore, due to the gas expanding into vacuum and therefore the pressure dropping rapidly the gas will

go through the process of rarefication, thus after some distance from the nozzle even continuum formulations break down. This will be discussed in more detail in chapter 3.6 where possible ways to formulate solutions using numerical techniques. [4]

3.2 Expected flow regimes

Continuum Regime

The whole Theory relies heavily on the continuum model. For every location of the flow, but the vacuum, it will be assumed that it suffices to approximate the state variables $(T,\ p, \rho)$ at certain locations using a simple continuum model presented in chapter 3.3 and use these state variables to calculate the Knudsen number.
A sensible question to ask at this point is, where in the flow is it most probable to encounter the highest Knudsen number. Because this will reduce the locations to check for high Knudsen numbers when other formulations to calculate the state variables are used and therefore will simplify the process. To find such most probable Location, starting from the Definition of the Knudsen number. [7, 4]

$$Kn(p,T) = \frac{\lambda}{L_c} = \frac{\mu(T)}{pL_c}\sqrt{\frac{\pi RT}{2}}$$

Where λ is the mean free path, L_c is the characteristic length, k_B is the Boltzmann constant, R is the specific gas constant, T is the temperature of the fluid, p is the pressure of the fluid, M_m is the molar mass and μ is the dynamic viscosity.
The dynamic viscosity can be calculated using Sutherland's formula. [13]

$$\mu(T) = \mu_0 \left(\frac{T}{T_0}\right)^{3/2} \frac{T_0 + S_\mu}{T + S_\mu} \tag{3.1}$$

Where mu_0 is the reference viscosity at the reference temperature T_0 and S_μ representing the Sutherland constant, whose values are dependent on the chosen gas. For nitrogen these have the following values [14]

$$S_\mu = 111\ K\ , \quad T_0 = 300.55\ K\ , \quad \mu_0 = 17,81\ \text{sPa}$$

Following plot shows the exact values using the Sutherland formula, plus two mean linear approximations in the range of 200-600 K, for the given values. One of them forcing the intercept to be zero. This will shift the values where Knudsen number reaches the continuum limit but won't have much influence on the behavior of the Knudsen number, thus version of the best-fit will be used for the following argument.

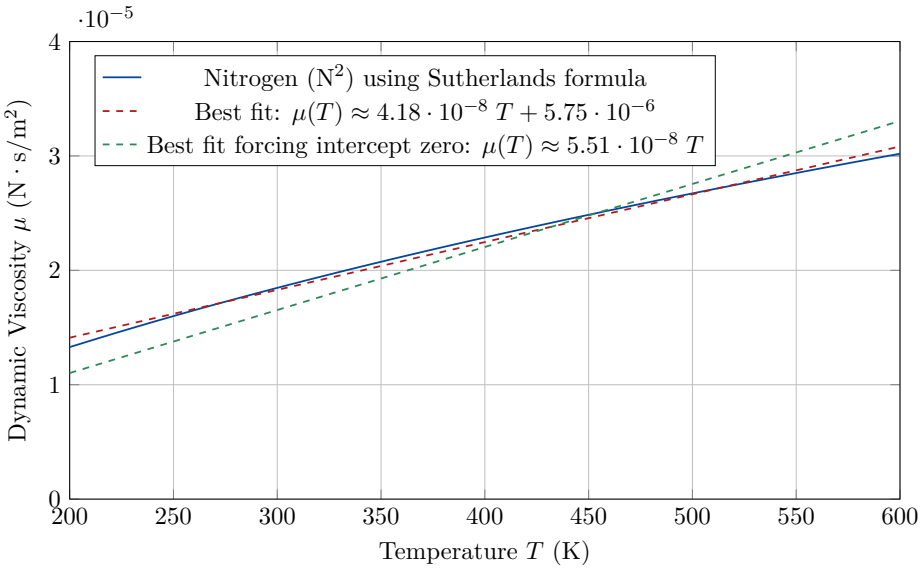

Figure 9: Values for the dynamic viscosity of nitrogen using the Sutherland formula, with addition of two square-error, best-fits of the Sutherland formula in the range of $200 < T < 600$, one with intercept being forced to zero.

Assuming L_c to be the throat diameter $A_{2,\,4} = 2 \cdot 10^{-6}$ m since this will cause the highest Knudsen number therefore a part of the system with a lower value of L_c will just reach transient flow sooner. Also by using the best-fit line with intercept forced zero with a slope of $k = 5.51 \cdot 10^{-8}\ \frac{\mathrm{sPa}}{\mathrm{K}}$ from the plot in figure 9 the Knudsen number can be reduced to a simple proportionality relation:

$$Kn(p,T) \approx \frac{k \cdot T}{L_c}\sqrt{\frac{\pi R}{2}} \cdot \frac{\sqrt{T}}{p} := \alpha \cdot \frac{T^{3/2}}{p} \quad \rightarrow \quad Kn \propto \frac{T^{3/2}}{p} \tag{3.2}$$

Using the simplification of $Kn(p,\ T)$ finding an approximate value of α for our case is possible:

$$\alpha = \frac{k}{L_c}\sqrt{\frac{\pi R}{2}} \rightarrow \alpha = \frac{5.55 \cdot 10^{-8}\frac{\mathrm{sPa}}{K}}{20 \cdot 10^{-6}\mathrm{m}}\sqrt{\frac{\pi 2.96 \cdot 10^{2}\frac{\mathrm{J}}{\mathrm{kgK}}}{2}} \approx 0.06\frac{\mathrm{Pa}}{\mathrm{T}^{3/2}}$$

Since α is now approximated, the pressures and temperatures can be determined where continuum flow in our system will most likely break down:

$$p_{\mathrm{trans}} = \alpha\frac{T^{3/2}}{Kn} \quad \text{where} \quad Kn = 0.1$$

Assuming temperature to be held constant at either 300 or 500 K, the corresponding pressure leading to a transition to molecular flow can be found.

$$T_{0,1} = 300\ \mathrm{K} \quad \rightarrow \quad p_{\mathrm{trans},1} = 0.03\ \mathrm{bar}$$
$$T_{0,2} = 500\ \mathrm{K} \quad \rightarrow \quad p_{\mathrm{trans},2} = 0.07\ \mathrm{bar}$$

Therefore, very low pressures are needed to bring the flow through our assembly to transition into molecular flow, but since the purpose of the reactor is to experiment at "high" pressures close to ambient, we can assume the flow to be continuum throughout the whole assembly.

But this still doesn't yet give a clear picture where in the assembly to expect the highest Knudsen number. But it already gives a clue that at a given temperature T, the only way the flow may reach low Knudsen numbers and transition to molecular flow is in regions with low pressure. To now pin down the most probable location for this to happen, the relation between pressure and temperature must be examined, since now continuum flow can be assumed, the changes in Temperature and pressure can be plotted over the Mach number. Since it is the main driving force for change in state variables in isentropic continuum flow.

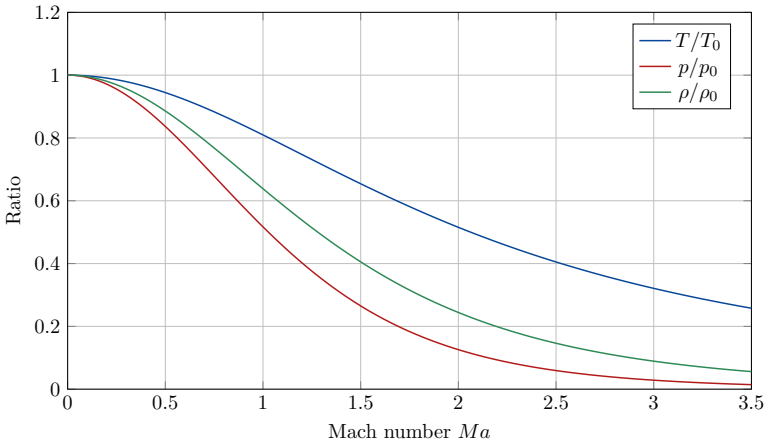

Figure 10: Isentropic temperature, pressure, and density ratios (equations (2.6) - (2.8)) as a function of Mach number for $\gamma = 1.47$.

From figure 10 it becomes clear that temperature changes less rapidly in relation to the Mach number. Thus, as long as the stagnation conditions of the system yield a Knudsen number which places the gas in the continuum regime, moving more towards molecular regime, always means accelerating the flow. Since flow in closed geometries usually are assumed to be subsonic inside and only surpass sonic velocities when exiting the geometry into an ambient pressure which is low enough to accelerate it over Mach one, now the location where a transition occurs becomes clear. It most likely starts at the exit plane of the outlet nozzle, moving further into the assembly as stagnation pressures are lowered.

Knudsen Number in low pressure Zones As the gas is leaving the outlet geometry and expands into the vacuum the characteristic length looses its significance. This is because the walls of the vacuum chamber are very far away in comparison to the length-scales of the flow geometry, while the gas expands it will lose pressure to conform to the vacuum and in that process will transition into free molecular flow. This leads to formulations using the mach number also loosing its significance. Therefore, it makes sense to identify a much more elegant way of calculating the local Knudsen number Kn_L which will be much more applicable in this situation.

$$Kn_L = \frac{\lambda}{\phi}\left|\frac{d\phi}{dx}\right| \tag{3.3}$$

Where λ is the mean free path, ϕ is some state variable of the flow. This way the Knudsen number can be calculated throughout the expansion of the gas and can be used to find the contour lines where the transition between continuum and molecular flow will happen. [15, 16, 10]

Laminar Flow

The Reynolds number itself does not bare any real significance for the applicability of the formulations used. Nonetheless, deviations in Reynolds number can in reality shape great parts of how the flow behaves and therefore effects important state variables.
Reynolds numbers per unit length for isentropic expansion range $10^{-2} < Re/l < 1$, whereas the characteristic length is constant at $L_c = 20 \cdot 10^{-6}$ and will therefore dominate the equation forcing low Reynolds numbers. [17]
Therefore the flow will stay laminar as long as it is contained inside the assembly and therefore mixing will be most likely diffusion mediated. [18]

Steady Flow

Steadiness of the flow is essentially given by the fact that the temperature T_0 and the pressure p_0 of the reservoir will be held constant during measurements. Thus, the flow will be driven by the pressure differential between the vacuum and the reservoir alone. So there is no reason for the flow to establish any dynamic behaviors after reaching some equilibrium state, after gas is first released into the system. This is true for regions inside as well as outside the assembly. [10]

3.3 One-dimensional isentropic variable area flow

By assuming the flow through the assembly will be fully isentropic and pseudo one-dimensional it is possible to calculate the state variables at every point knowing the stagnation conditions and the ratio between the cross-sectional area at the point of interest A_i and the at throat of the assembly A^*.
It must be noted that this is a very radical approximation since for the flow to be considered pseudo one-dimensional the problem must be reduced to consist purely of variable area ducts. This clearly overlooks the fact that when entering and leaving the reactor the gas has to perform a right angle turn to follow the flow path. Another constraint on the duct geometry to achieve reasonable solutions assuming pseudo one-dimensional flow is that the duct must change its cross-sectional area gradually. [4] This won't be the case inside the reactor, since there is no way of slicing the reactor chamber to achieve a gradual change in cross-section, especially around the inlet and outlet.

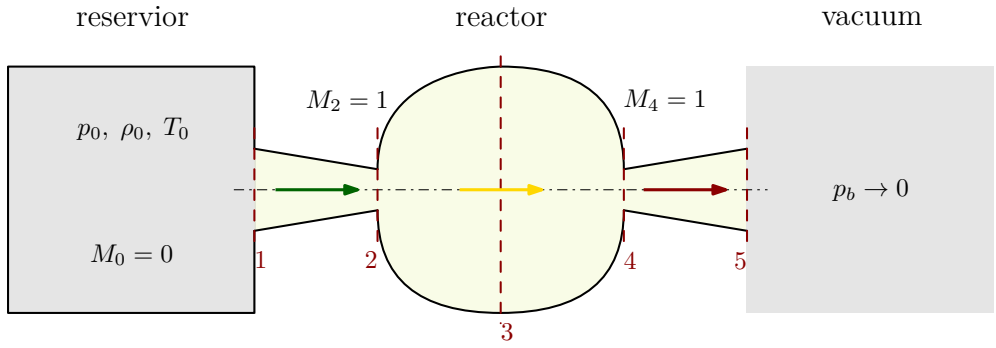

Figure 11: Idealized geometry of the reactor assembly modeled as a one-dimensional variable-area duct. The yellow region represents the domain where quasi one-dimensional isentropic flow is assumed (as described in section 3.1). Grey indicates stagnant gas, green arrow indicates subsonic flow at the inlet, and the red arrow indicates supersonic flow at the outlet. Flow in the central reactor region is most likely slow-moving.

This geometry can now be characterized as a double throat, and therefore one-dimensional isentropic flow will yield one of in two fundamental solutions. Depending on how the steady state in the system is reached, flow velocity of the stream will either stay subsonic and therefore decrease when entering the reactor or become sonic at the throat (2) and continue to accelerate. Other non-trivial solutions won't be discussed. [19, 11]

Calculations

The first step is to define the critical locations, where the flow fill be chocked. Since the outlet is expanding into vacuum, resulting in a pressure ratio tending towards zero, therefore the flow therefore must be chocked and can be recognized as a critical point. Maximum mass-flow occurs if the flow is chocked. Therefore, to keep up with the mass-flow of the outlet, the inlet must also be chocked:

$$A_{2,4},\ p_{2,4},\ \rho_{2,4},\ T_{2,4} \quad \xrightarrow{Ma=1} \quad A^*,\ p^*,\ \rho^*,\ T^*$$

The second reference location corresponding to the stagnation or total conditions is at the entry of the inlet nozzle (1), which can be defined afterward to get quantitative solutions.

$$A_1,\ p_1,\ \rho_1,\ T_1 \quad \xrightarrow{Ma=0} \quad A_0,\ p_0,\ \rho_0,\ T_t$$

Next step is to take the cross-sectional areas A_i at every point i defined in chapter 3.1, and calculate their ratios to the throat area $A_{2,\,4}$. To use them for solving equation (2.5) relating mach number and area-ratio $\frac{A^*}{A_i}(Ma)$, numerically yielding one subsonic and one supersonic solution depending on the initial condition given to the solver in appendix A.2.2.

Afterward the ratio of the local state variables to the total conditions can be determined using equations (2.6) - (2.8), which can be used, after defining the total conditions of the system, to calculate the local variables for every point.

i	$\frac{A_i}{A^*}$	M	$\frac{p_i}{p_t}$	$\frac{\rho_i}{\rho_t}$	$\frac{T_i}{T_t}$	description
1	4	0	1	1	1	reservoir conditions
2	1	1	0.52	0.64	0.81	inlet nozzle exit
3	318.31	∼0	∼1	∼1	∼1	center of the reactor-volume
		10.55	$3.28 \cdot 10^{-5}$	$8.90 \cdot 10^{-4}$	$3.68 \cdot 10^{-2}$	
4	1	1	0.52	0.64	0.81	outlet nozzle inlet
5	4	0.15	0.98	0.99	0.99	outlet nozzle exit ≠ vacuum conditions
		3.06	0.03	0.08	0.31	

Table 1: Isentropic flow properties at various locations along the flow path, assuming fully one-dimensional isentropic conditions throughout the system (calculations: appendix A.1). Both values are mathematically valid; green highlights the more physically likely solution, whereas red denotes the less likely one, described in more detail in the interpretation paragraph.

Now knowing the approximate way state variables change inside the system, the assumption taken in chapter 3.2 regarding the Reynolds and Knudsen number can be tested for the following values. With the mass flow being conserved throughout the system it can be calculated from equation (2.10) using given stagnation conditions and any pair of cross-sectional area and mach number Ma at some point i.

$$p_{0,\,1} = 1.5 \text{ bar} \qquad T_{0,1} = 300 \text{ K} \qquad \text{at} \qquad \dot{m}_1 \approx 1.1 \cdot 10^{-7} \ \frac{\text{kg}}{\text{s}}$$

$$p_{0,\,2} = 1.5 \text{ bar} \qquad T_{0,2} = 500 \text{ K} \qquad \text{at} \qquad \dot{m}_2 \approx 8.5 \cdot 10^{-8} \ \frac{\text{kg}}{\text{s}}$$

Additionally, the lower limit for the reservoir pressure $p_{0,\,min}$ where some part of the system transitions to the molecular regime, will be determined. Again for temperatures $T_{0,\,1},\ T_{0,\,2}$

	T_t	1	2	3 (sub)	3 (sup)	4	5 (sub)	5 (sup)
Re	300 K	-	0.0001	0.4	∼ 0	0.0001	0.005	0.0002
	500 K	-	0.001	0.8	0.0001	0.001	0.01	0.0005
Kn	300 K	0.001	0.002	0.001	0.2	0.002	0.001	0.009
	500 K	0.002	0.003	0.002	0.02	0.003	0.002	0.02

Table 2: Knudsen and Reynolds numbers for $p_0 = 1.5\,\text{bar}$ and $T_0 = 300, 500\,\text{K}$ using values from table 1. The cell highlighted red indicates a transitional regime, whereas the titles colored red and green correspond to the less and more likely solutions from table 1 respectively

It now becomes clear that the assumptions made in chapter 3.2 are accurate:

- Slip on the boundaries is to expect.
- The Mach number has major influence on the value of the Knudsen number, thus high Mach numbers point to possible transition to molecular regime. This will most likely only happen at the outlet nozzle exit if stagnation pressure is low enough.
- The outlet always corresponds to the highest Knudsen number with exception to the hypersonic solution found in the middle of the reactor. Which corresponds to a mathematically true but physically most likely impossible solution as described previously.
- Disregarding the non-physical solutions, the flow through the assembly will be in continuum regime with slip boundary condition.
- Reynolds numbers are very low, therefore no turbulences are expected.

Interpretation

The equation relating area ratio and Mach number has in general two solutions. This leads to the two solutions for every point which is not defined as a (total or critical) reference point will have mathematically true solutions One corresponding to subsonic flow and the other one to supersonic flow, which of those are applicable in the situation is to decide.

For the outlet it is easier to discern since when exhausting into a vacuum the flow will be forced supersonic. This is expected even tho there is actually no specific converging section when leaving the reactor, especially if the reactor is seen as a reservoir by itself, like it will in chapter 3.5. In short, the flow itself when flowing over the edge of a sudden contraction in the flow geometry, can itself form a kind of converging section and still accelerate to sonic conditions. This will be discussed in the next chapter in more detail.

While the above analysis provides a baseline using one-dimensional isentropic flow, real micro-channels often experience additional effects such as slip at the boundaries and non-negligible viscous losses. These phenomena can significantly alter the flow, especially at small scales. The next section therefore examines such microchannel-specific behaviors and their impact on the flow assumptions made so far.

3.4 Flow behaviors in micro-channels

Going from macro scale channels to microscales has some major implications for the behavior of the gas. The primary factor for these differences is slipping at the boundary of the surfaces. This is due to the fact that at small characteristic length scales the Knudsen number (Kn), whose value describes the interaction of the molecules in the gas and its boundaries, becomes relatively high ($Kn > 0.001$). Which usually puts the gas flow in the category of compressible flow with slip at the boundaries.

Most of these behaviors have to be studied using complex simulations or experimental results and are sometimes not fully explained. Therefore, this section is not intended to give concrete definitions or formulations, but to provide as many relevant references regarding behaviors in microfluidics as possible. It will be mainly based on the review study conducted by Amit Agrawal in 2011.

Phenomenon of Slip

Slip, in comparison to non-slip, refers to the fact that the tangential velocity close to a surface is non-zero. Maxwell suggested that on a control surface s, at distance half the mean free path away from the surface, one half of the molecules come in from one mean free path away with the tangential velocity u_λ, the other half is reflected from the surface. Assuming a fraction σ of the molecules are reflected diffusively (average velocity corresponds to velocity at the wall u_w)at the walls, with the remainder $(1-\sigma)$ being reflected specularly (no change in their impinging velocity u_λ). When expanding u_λ in a second order Taylor series this yields the second order slip boundary condition used in continuum analysis:

$$u_g - u_w = \left[\frac{2-\sigma}{\sigma} Kn \left(\frac{\partial u}{\partial n}\right)_s + \frac{Kn^2}{2}\left(\frac{\partial^2 u}{\partial n^2}\right)_s\right] \tag{3.4}$$

Where u stands for the streamwise velocities, where the subscripts g, w and s refer to gas, wall and control surface, with n being the normal to the control surface. And most importantly σ is the tangential momentum accommodation coefficient, or short TMAC.

Determining the TMAC for a specific application is one of the most critical aspects when dealing with slip conditions, as it directly influences the velocity slip at the gas-wall interface and, consequently, the overall behavior of rarefied gas flows. This is usually achieved through empirical studies or simulations like direct simulation Monte Carlo which will be discussed in more detail in the next section.

Sudden expansion or contraction

When the flow exits a confined duct into the reactor, the geometry no longer resembles a uniform channel but rather a sudden expansion or contraction. Agrawal shows that in such cases the assumption of strict isentropic behavior breaks down as the abrupt change in cross-section induces local flow separation, vena contracta effects, and additional losses. These non-isentropic phenomena lead to variations in the stagnation conditions downstream; the static pressure and temperature no longer remain uniquely determined by the inlet conditions but adjust in response to the complex expansion dynamics. By considering the reactor as a reservoir with its own stagnation state, the analytical formulation accommodates the changes introduced by the sudden geometric transitions. In this formulation, the mass flow entering and exiting the reactor is governed not only by the duct geometry but also by the additional pressure losses and momentum deficits associated with the rapid expansion or contraction.

Surface Roughness

Similarly, surface roughness plays a critical role in modifying the effective slip conditions at the channel walls, as detailed by Agrawal (2011). At the microscale, even minor deviations from a smooth surface can lead to enhanced momentum exchange between the gas and the wall, effectively reducing the local slip length compared to that predicted by the ideal Maxwell model. This increased friction at the wall alters the pressure distribution and thus the stagnation conditions within the flow. In the context of the reactor-reservoir model, the presence of surface roughness must be accounted for by modifying the boundary conditions to reflect the non-ideal accommodation of tangential momentum. Incorporating roughness effects—either through empirical corrections or higher-order slip models—allows for a more realistic prediction of the flow behavior, particularly in regions where the geometric changes force deviations from the classical isentropic relations.[20, 21]

3.5 Including non-isentropic behaviors

In section 3.3 the flow is assumed to be fully isentropic and one-dimensional. This led to the simplification of the reactor being a variable area duct, which leads to a change in state-variables along the path of the gas flowing from the inlet to the outlet. Since this change is based on the variable area duct formulation, it won't represent an accurate solution for the given geometry. The leak is located at the perimeter of the reactor, which is not an actual location in this formulation. To be able to include the influence of the leak analytically, without using numerical tools, further simplification is needed.

In section 3.4 some phenomenons occuring in micro channels are mentioned, which are hard to account for in analytical calculations. Thus, this section will explore a formulation of the system, where both the inlet reservoir and the reactor are assumed to be reservoirs, with stagnation conditions associated with them. In turn disconnecting the two reservoirs and resulting in two independent problems, describing gas from a reservoir flowing into a discharge region with a given back pressure. Representing a change in stagnation conditions which can be attributed to non-isentropic processes happening while the gas enters or leaves the reactor.

Now proper assumptions have to be taken to connect both reservoirs again. At first without including the leak. Stagnation conditions for the reactor are chosen, resulting in a mass-flow at the outlet. Which in turn have to be compensated by the inlet, now without forcing sonic conditions at the throat of the inlet. Through choosing the back-pressure of the reservoir to be the total pressure of the reactor a connection is established. But to be able to solve the system, at least one other value of a state variable in the system of the reservoir has to be assumed. Two possible assumptions for Temperature are presented in the following paragraphs.

Afterward, the influence on the inlet mach number M_2 of additional mass flow $\dot{m}_L$ leaving the reactor is inspected. Trying to find an upper limit for mass flow through the leak, after which the inlet is again forced to reach sonic flow speeds, without having to derive an explicit way to calculate $\dot{m}_L$.

Formulations without including the leak

In the absence of a leak, the system reduces to a single flow path from the inlet reservoir, through the reactor volume, and out to the vacuum. All mass entering the reactor must exit via the outlet nozzle, eliminating any additional flow paths. Consequently, the boundary conditions become simpler, and standard relationships between the inlet and reactor stagnation states can be applied directly. This section formulates those relationships and illustrates how isentropic or isothermal assumptions may be used without the complexities introduced by a leak.

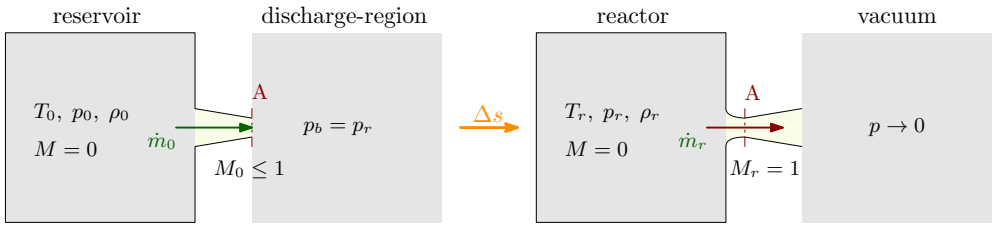

Figure 12: Idealized system separating the reactor from the inlet and outlet regions to account for non-isentropic effects. The yellow regions represent domains where one-dimensional flow is assumed. Grey indicates stagnant gas, green arrow indicates subsonic flow, and the red arrow indicates supersonic flow at the outlet. An entropy change Δs occurs between the gas flowing into the discharge region and the reactor, and the converging section at the outlet represents the flow constraining itself as it accelerates as mentioned in 3.1.

Since this still constitutes a closed system, mass flow must be conserved, thus:

$$\dot{m}_0 = \dot{m}_r = const.$$

The reactor still discharges into vacuum, this therefore must lead to chocked flow:

$$M_r = 1$$

From the geometry in section 3.1 it is given that:

$$A_0 = A_r = A$$

The mass flow rates from the reactor into vacuum, can be calculated using the isentropic mass flow equation (2.10)
Reservoir → Reactor

$$\dot{m}_0 = A\, p_0 \sqrt{\frac{\gamma}{RT}}\, M_0 \left(1 + \frac{\gamma - 1}{2}\, M_0^2\right)^{-\frac{\gamma+1}{2(\gamma-1)}} \tag{3.5}$$

Reactor → Vacuum

$$\dot{m}_r = A\, p_r \sqrt{\frac{\gamma}{RT}} \left(1 + \frac{\gamma - 1}{2}\right)^{-\frac{\gamma+1}{2(\gamma-1)}} \tag{3.6}$$

Thus from ($\dot{m}_r = \dot{m}_0 = const.$)

$$A\, p_r \sqrt{\frac{\gamma}{RT}} \left(1 + \frac{\gamma - 1}{2}\right)^{-\frac{\gamma+1}{2(\gamma-1)}} = A\, p_0 \sqrt{\frac{\gamma}{RT}}\, M_0 \left(1 + \frac{\gamma - 1}{2}\, M_0^2\right)^{-\frac{\gamma+1}{2(\gamma-1)}}$$

Which constitutes the general conservation of mass equation for the system without connecting the state variables of the reservoirs in any way. This will be the starting point for both of the following approaches.

Isentropic approach In this approach, the reactor is treated as a downstream reservoir with distinct stagnation conditions, implying that irreversibilities have occurred somewhere in the flow path. Instead of modeling the associated entropy generation, local isentropic relations are used to connect the inlet reservoir's stagnation state to the reactor boundary. This method effectively embeds any non-isentropic effects into a "shift" in stagnation values, so the reactor's reduced pressure and/or temperature serve as an isentropic back condition. As a result, flow properties in the nozzles or ducts can still be obtained from standard one-dimensional isentropic equations, even though the actual flow inside the reactor may be more complex.

$$T_b = T_r \quad \rightarrow \quad T_0 = T_r \left(1 + \frac{\gamma - 1}{2} M_0^2\right)$$

and

$$p_b = p_r \quad \rightarrow \quad p_0 = p_r \left(1 + \frac{\gamma - 1}{2} M_0^2\right)^{\frac{\gamma}{\gamma - 1}}$$

Assuming the conditions of the discharge region to match the values in the reactor and using the isentropic relations to express T_0 and p_0 in terms of T_b and P_b the previously defined conservation of mass equation yields:

$$A\, p_r \sqrt{\frac{\gamma}{R\, T_r}} \left(1 + \frac{\gamma - 1}{2}\right)^{-\frac{\gamma+1}{2(\gamma-1)}}$$

$$=$$

$$A\, p_r \left(1 + \frac{\gamma - 1}{2} M_0^2\right)^{\frac{\gamma}{\gamma-1}} \sqrt{\frac{\gamma}{R\, T_r}} \left(1 + \frac{\gamma - 1}{2} M_0\right)^{-\frac{1}{2}} M_0 \left(1 + \frac{\gamma - 1}{2}\, M_0^2\right)^{-\frac{\gamma+1}{2(\gamma-1)}}$$

Canceling out variables present on both sides and combining the potential expressions on the right side it results a function of M_0 only dependent on γ, since the summing the exponents equals zero.

$$M_0 = (1 + \frac{\gamma - 1}{2})^{-\frac{\gamma+1}{2(\gamma-1)}} = 0.57 \quad \text{for} \quad \gamma = 1.47$$

Thus resulting in following ratios between the conditions in the reactor and the reservoir.

$$\frac{T_r}{T_0} = 0.93\,, \quad \frac{p_r}{p_0} = 0.79\,, \quad \frac{\rho_r}{\rho_0} = 0.85\,, \quad \dot{m} = 7.0 \cdot 10^{-8}\ \frac{\text{kg}}{\text{s}}$$

Constant temperature approach The isothermal approach similarly separates the reactor as an independent reservoir, but enforces a uniform temperature shared with the inlet reservoir. Despite holding temperature constant, a pressure difference can still arise, which inherently indicates a net entropy change. This scenario is plausible if the reactor walls maintain a uniform thermal environment, allowing the gas to remain at the same temperature while the pressure drops. The resulting non-isentropic behavior is thus represented by a constant-temperature boundary condition, and simpler local flow equations remain usable, provided the irreversibilities are captured in the overall pressure imbalance between inlet and reactor.

$$T_r = T_0 = T$$

This approach is going contrary to isentropic formulation, but still seems somehow plausible due to the fact that the gas in the reservoir just like the whole assembly will be preheated to a certain temperature. Since for small cavities the surface area of its walls is much larger in proportion to its internal volume, heat transfer from the walls will be significant even without high mixing due to low Reynolds numbers present in microfluidics.

$$p_r \left(\frac{2}{\gamma+1}\right)^{\frac{\gamma+1}{2(\gamma-1)}} = p_0\, Ma_0 \left(1+\frac{\gamma-1}{2}\, Ma_0^2\right)^{-\frac{\gamma+1}{2(\gamma-1)}}$$

Again using the isentropic relation (2.7) for p_0

$$p_r \left(\frac{2}{\gamma+1}\right)^{\frac{\gamma+1}{2(\gamma-1)}} = p_r \left(1+\frac{\gamma-1}{2} Ma_0^2\right)^{\frac{\gamma}{\gamma-1}}\, Ma_0 \left(1+\frac{\gamma-1}{2}\, Ma^2\right)^{-\frac{\gamma+1}{2(\gamma-1)}}$$

Rearranging leads to an equation only dependent on γ and the mach number Ma_0 at the inlet.

$$\left(\frac{2}{\gamma+1}\right)^{\frac{\gamma+1}{2(\gamma-1)}} = Ma_0 \left(1+\frac{\gamma-1}{2}\, Ma_0^2\right)^{\frac{1}{2}}$$

Which can be solved analytically, since by squaring both sides and rearranging it resembles a simple quadratic equation:

$$Ma^4 + \frac{2}{\gamma-1} Ma_0^2 - \frac{2}{\gamma-1}\left(\frac{2}{\gamma+1}\right)^{\frac{\gamma+1}{\gamma-1}} = 0 \tag{3.7}$$

Now substituting $Ma_0^2 = f \quad \rightarrow \quad Ma_0 = \sqrt{f}$

$$f = -\frac{1}{\gamma-1} \pm \sqrt{\frac{1}{(\gamma-1)^2} + \frac{2}{\gamma-1}\left(\frac{2}{\gamma+1}\right)^{\frac{\gamma+1}{\gamma-1}}} \tag{3.8}$$

There is only one real solution for this equation using the positive square root. For $\gamma = 1.47$ we get the solution:

$$f = 0.31 \quad \rightarrow \quad Ma_0 = 0.55$$

Which corresponds to the following ration between the conditions in the reactor and the reservoir, which results in the given mass-flow:

$$\frac{T_r}{T_0} = 0.93\,, \quad \frac{p_r}{p_0} = 0.80\,, \quad \frac{\rho_r}{\rho_0} = 0.86\,, \quad \dot{m} = 6.8 \cdot 10^{-8}\ \frac{\mathrm{kg}}{\mathrm{s}}$$

at reservoir conditions of $T_0 = 500$ K and $p_0 = 1.5$ bar. Which is in the same order of magnitude as the mass-flow for the fully isentropic formulation in Section 3.3. The discrepancy in mass-flow can be attributed to the change in entropy, indicated by the change in stagnation conditions.

Formulations including the leak

Including the leak can now be achieved by assuming additional mass flow out of the reactor, the inlet now has to compensate.

$$\dot{m}_0 = \dot{m}_r + \dot{m}_L \quad \rightarrow \quad \dot{m}_L = \dot{m}_0 + \dot{m}_r$$

This forces the total conditions of the reservoir to increase in order to keep the conditions in the reactor the same. Therefore, increasing the Mach number until a critical ratio (2.9) is reached, and the flow becomes sonic at the throat of the inlet.

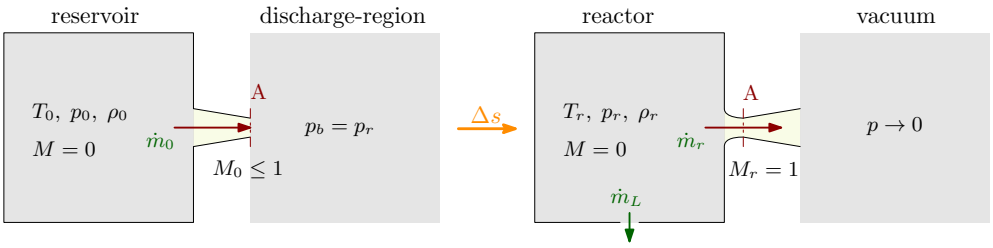

Figure 13: Idealized system separating the reactor from the inlet and outlet regions to account for non-isentropic effects, now including a leak path from the reactor. The yellow regions represent domains where one-dimensional flow is assumed, gray indicates stagnant gas and the red arrows indicate supersonic flow. An entropy change Δs occurs between the discharge region and the reactor, and the converging section at the outlet represents the flow constraining itself as it accelerates, as mentioned in Section 3.1

Using isentropic mass flow equations this is described by assuming both mach numbers to be one in equation (3.5) and (3.6).

$$\dot{m}_L = A\,p_0 \sqrt{\frac{\gamma}{RT}} \left(1 + \frac{\gamma - 1}{2}\right)^{-\frac{\gamma+1}{2(\gamma-1)}} - A\,p_r \sqrt{\frac{\gamma}{RT}} \left(1 + \frac{\gamma - 1}{2}\right)^{-\frac{\gamma+1}{2(\gamma-1)}}$$

To express the temperature T_0 and pressure p_0 of the reservoir in terms of the conditions in the reactor, it will again be assumed the conditions in the discharge-region and the reactor match. This formulation is chosen due to the fact that it yielded a higher Mach number for the inlet, thus will reach sonic conditions first. Therefore, representing the "worst case" in the sense that it yields the lowest amount of mass flow needed to force the inlet sonic. After inserting the isentropic ratios and rearranging the equation yields:

$$\dot{m}_L = Ap_r \sqrt{\frac{\gamma}{RT_r}} \cdot \left(1 + \frac{\gamma - 1}{2}\right)^{-\frac{\gamma+1}{2\,(\gamma-1)}} \tag{3.9}$$

Assuming again the reservoir conditions to be $p_0 = 1.5$ bar and $T_0 = 500$ K which can be used to calculate the reservoir conditions using the critical ratios mentioned in Section 2.5. The additional mass-flow through the leak, leading to sonic conditions at the inlet throat can be calculated.

$$\dot{m}_L = 3.6 \cdot 10^{-8}\ \frac{\text{kg}}{\text{s}}.$$

Which is around half of the mass-flow calculated for the disconnected reservoirs. Thus, it can be concluded that if the mass-flow through the leak is comparable to the mass-flow through the outlet, this will lead to the inlet throat going sonic, which could lead to a major change in behavior of the gas after leaving the inlet, like shock-waves and rapid changes in state-variables.

Since this still would constitute a coupled system, where the leak influences the outlet through for example pressure drops and also the other way around, the exact distribution of mass-flow between the two and also the reservoir conditions at which the inlet goes sonic have to be explored further through simulation.

3.6 Under-expanded nozzle plume at outlet

Once the gas emerges from the reactor and enters the outlet nozzle, it undergoes a rapid expansion into a low-pressure or near-vacuum environment. This regime differs significantly from the upstream flow: velocity increases dramatically, density drops, and shock formations or rarefaction waves can appear. The one-dimensional isentropic models used until now cannot fully capture these effects, especially if there is phase change (e.g., condensation) or a transition to free-molecular flow. Hence, more advanced modeling approaches are required. [12, 4]

Method of characteristics

Ideal nozzle design The method of characteristics is a mathematical technique used to design supersonic nozzles so that gas flows expand smoothly from sonic to supersonic speeds without generating internal shocks. It works by tracing characteristic lines—paths along which flow properties remain constant—through the nozzle region. By aligning the walls with these lines it ensures that each incremental flow turn occurs through a series of controlled expansion waves, rather than abrupt angle changes that could cause shocks. If fully expanded this leads to a straight column of gas leaving the nozzle, where all of its energy is converted into kinetic energy without significant losses due to shocks. [22, 23]

Determining flow field for free expansion Mach lines are a concept usually encountered in 2-D supersonic flows (i.e. $M > 1$). They are a pair of bounding lines which separate the region of disturbed flow from the undisturbed part of the flow. These lines occur in pairs and are oriented at an angle $\mu = \arcsin\left(\frac{1}{M}\right)$ (the Mach angle) with respect to the direction of motion. In a 3-D flow field, these lines form a Mach cone, whose half-angle is the Mach angle itself.

In an under-expanded jet, the method of characteristics can also be applied immediately downstream of the nozzle exit to predict the initial spread of the flow. It does this by mapping local Mach numbers and density profiles along characteristic lines, thus giving a first approximation for velocity and pressure distributions.

In supersonic expansions, Prandtl–Meyer expansion fans define the maximum turning angle θ_{max} the gas can undergo around a sharp corner. Which can be calculated using the following equation:

$$\theta_{max} = \nu_{max} - \nu(Ma)$$

$$\theta_{max} = \frac{\pi}{2}\left(\sqrt{\frac{\gamma+1}{\gamma-1}} - 1\right) - \sqrt{\frac{\gamma+1}{\gamma-1}}\arctan\sqrt{\frac{\gamma-1}{\gamma+1}(Ma^2-1)} + \arctan\sqrt{Ma^2-1} \tag{3.10}$$

Where $\nu_max, \nu(Ma)$ are the Prandl-Meyer functions, Ma is the mach number before the turn and γ is the ratio of heats for the given gas. By incorporating these fans, the method of characteristics predicts the outer boundary of the flow—effectively identifying the angle outside which the density and mass flux become negligible. This angle is critical for determining the lateral extent of the under-expanded plume and for estimating where essentially all of mass flow is confined. Using equation (3.10) for the mach number at the outlet nozzle exit calculated in section 3.3 the maximum turning angle yields:

$$\theta_{max} = 68.9° \qquad \text{for} \qquad Ma = 3.06\,, \quad \gamma = 1.47$$

Notably, findings from Cassanova and Stephenson [24] — even though the nozzle half-angle does not match — still offer valuable reference points regarding expansion ratios

and associated flow features. However, a key limitation arises if condensation or other non-ideal processes occur. Experiments show that for working fluids like nitrogen, condensation in the expansion region can alter the thermodynamic state and produce deviations from these idealized solutions. Consequently, while the method of characteristics remains valuable for nozzle design and near-exit expansions, it cannot fully capture condensation effects or strong rarefaction phenomena further downstream. [12, 25, 26]

Navier-Stokes Equations

A second option is to solve the Navier–Stokes equations numerically, using no-slip or first/second-order slip boundary conditions as appropriate. Near the nozzle exit—where the flow is still predominantly continuum—Navier–Stokes simulations can provide detailed velocity and pressure fields, including shock structures and boundary-layer effects. As the gas expands and its density decreases, however, continuum assumptions start to break down. While slip or transitional models can extend the validity range, ultimately they cannot fully describe the molecular-level interactions that dominate in highly rarefied regions. Consequently, beyond a certain distance from the nozzle exit or under conditions favorable to partial condensation, Navier–Stokes solutions must be supplemented by more advanced kinetic-based methods. [27, 4]

Direct simulation Monte Carlo (DSMC)

To address the shortcomings of both the method of characteristics (under non-ideal conditions) and Navier–Stokes (when rarefaction becomes significant), the Direct Simulation Monte Carlo (DSMC) method is indispensable. DSMC performs a stochastic simulation of molecular motion and collisions, making it particularly well suited for:

- Transitional Regimes: Where the mean free path is comparable to or larger than the nozzle scale, DSMC accurately captures Knudsen-layer effects and velocity-slip phenomena.
- Condensation Phenomena: By including collision physics and intermolecular potentials, DSMC can handle the onset of condensation or two-phase flow more reliably than continuum or purely isentropic approaches. [11]
- Free Expansion: As the jet spreads into the vacuum and transitions toward free-molecular flow, DSMC seamlessly handles extremely high Mach numbers and very low densities, maintaining physical fidelity across a wide range of Knudsen numbers.

Although more computationally expensive than continuum-based methods, DSMC provides the most robust depiction of outlet flows—particularly for condensable gases like nitrogen—and ensures high accuracy from near-nozzle regions all the way to the fully rarefied state. [6, 28]

Summary

Overall, while the method of characteristics remains a cornerstone of ideal nozzle design and near-exit expansions (including the prediction of Prandtl–Meyer fans and maximum turning angles), condensation and severe rarefaction invalidate its purely isentropic assumption further downstream. Navier–Stokes simulations can capture intermediate regimes near the exit, but eventually fail in the highly rarefied or partially condensed flow domain. For a comprehensive treatment of under-expanded plumes—particularly with nitrogen or other condensable working fluids—the DSMC technique offers the necessary level of detail, bridging the gap from continuum flow at the nozzle exit to free-molecular flow far downstream.

Discussion

The analytical work presented in this thesis has provided a basic understanding of gas flow behavior within the micro-reactor assembly. Starting with the detailed geometrical characterization in Section 3.1, we simplified the reactor's complex structure into discrete segments—reservoir, inlet/outlet nozzles, and the central reaction volume—to enable a quasi one-dimensional approximation. This initial abstraction set the stage for applying isentropic flow theory and provided a baseline for estimating characteristic lengths and flow areas.

In Section 3.2, the expected flow regimes were determined by calculating key dimensionless numbers. The analysis revealed that, under typical operating conditions, the system predominantly falls within the continuum regime with slip at the walls. This finding is crucial because it validates the use of continuum-based formulations for the majority of the flow, while also pointing to specific zones (e.g., near the outlet) where the transition to molecular flow might occur.

Section 3.3 delved into one-dimensional isentropic variable area flow, where state variables were linked to changes in cross-sectional areas along the flow path. Although two mathematically viable solutions emerged—corresponding to subsonic and supersonic branches—the physical reasoning, supported by the geometry and boundary conditions, guided the selection of the more likely scenario. This process underscored the importance of aligning mathematical models with realistic operating constraints.

The discussion then moved to the microscale in Section 3.4, addressing flow behaviors in micro channels. Here, factors such as slip effects, surface roughness, and sudden geometric expansions were discussed qualitatively. These effects, which become significant as the characteristic lengths shrink, hint at deviations from classical isentropic behavior and suggest that empirical corrections or advanced simulation techniques may be necessary for a more accurate description.

Recognizing these limitations, Section 3.5 extended the analysis to include non-isentropic behaviors. By treating the reservoir and the reactor as distinct entities with independent stagnation conditions, the approach captured the impact of leaks and pressure losses on the overall mass flow. Although this formulation introduces further approximations, it serves to bridge the gap between idealized isentropic models and the more complex reality of the system.

Finally, Section 3.6 addressed the under-expanded nozzle plume at the outlet, where rapid expansion, shock structures, and rarefaction effects dominate. The discussion here emphasized that while traditional one-dimensional models offer a first approximation, advanced methods such as the method of characteristics, Navier–Stokes simulations, or DSMC are required to capture the full complexity of the free expansion into vacuum.

Conclusion

Symbols and Notation

Primary Symbols and Definitions

a speed of sound
A cross-sectional area of a duct
ρ mass density
c_p specific heat at constant pressure
c_v specific heat at constant volume
h enthalpy per unit mass, $u + pv$
L_c characteristic length
M Mach number, $\frac{V}{a}$
p pressure
q dynamic pressure, $\frac{\rho V^2}{2}$
R gas constant
s entropy per unit mass
T absolute temperature
u internal energy per unit mass
v specific volume, $\frac{1}{\rho}$
u velocity components parallel to flow
v velocity components perpendicular to flow
V speed of flow
V_∞ maximum speed at absolute zero
β $\sqrt{M^2 - 1}$
γ $\frac{c_p}{c_v}$ (ratio of specific heats)
θ shock-wave angle from upstream direction
μ Mach angle, $\sin^{-1} \frac{1}{M}$
μ absolute viscosity
ν Prandtl-Meyer angle

Subscripts

∞	free-stream conditions
0	total/stagnation conditions
$*$	critical conditions (local speed equals local speed of sound)
perf	thermally and calorically perfect gas
therm perf	thermally perfect, calorically imperfect gas

Notations

`[perf]`	thermally and calorically perfect gas.
`[therm perf]`	thermally perfect but calorically imperfect gas.
`[isen]`	isentropic flow process (not valid for shock waves).
`[adiab]`	adiabatic process (no heat transfer, may or may not be isentropic).

Formulary

This formulary gathers the key equations used in your thesis on micro-reactor gas dynamics. Only the most important, frequently referenced equations are included, with some additional useful relations used to derive some of the given equations.

Thermodynamics

- **Thermal Equation of State:** An equation of state relates pressure, specific volume, and temperature:
$$p = p(v, T)$$
- **Ideal Gas Law (Thermally Perfect):**
$$p = \rho R T \quad \texttt{[therm perf]}$$
- **1D Euler Equation (for a perfect gas):**
$$\frac{1}{\rho}\, dp + V\, dV = 0 \quad \texttt{[therm perf]}$$

Control Volume Analysis

- **Continuity Equation:**
$$\frac{d}{dt}\int_V \rho\, dV + \int_S \rho\, \vec{V} \cdot d\vec{A} = 0$$
For steady, one-dimensional flow (constant cross-sectional area):
$$\sum \rho\, V\, A = 0$$

Continuous One-Dimensional Flow

- **Speed of Sound:**
$$a = \sqrt{\left(\frac{\partial p}{\partial \rho}\right)_s} = \sqrt{\gamma\, \frac{p}{\rho}} = \sqrt{\gamma\, R T} \quad \texttt{[therm perf]}$$
- **Mach Number:**
$$Ma = \frac{V}{a} \quad (2.4)$$
- **Area-Mach Relation (Isentropic Flow):**
$$\frac{A}{A^*} = \frac{1}{Ma}\left[\frac{2}{\gamma+1}\left(1 + \frac{\gamma-1}{2} Ma^2\right)\right]^{\frac{\gamma+1}{2(\gamma-1)}} \quad \texttt{[isen, perf]} \quad (2.5)$$
- **Isentropic Relations:** From the constant p/ρ^γ we obtain:
$$\frac{p}{p_0} = \left(\frac{\rho}{\rho_0}\right)^\gamma = \left(\frac{T}{T_0}\right)^{\frac{\gamma}{\gamma-1}} = \left(\frac{a}{a_0}\right)^{\frac{2\gamma}{\gamma-1}} \quad \texttt{[isen, perf]}$$
- **Bernoulli's Equation for Compressible Flow:**
$$\frac{\gamma}{\gamma-1}\left(\frac{p_0}{\rho_0}\right)^{\frac{\gamma-1}{\gamma}}\left(\frac{p}{p_0}\right)^{\frac{1}{\gamma}} + \frac{V^2}{2} = \frac{\gamma}{\gamma-1}\frac{p_0}{\rho_0} \quad \texttt{[isen, perf]}$$

- **Stagnation/Total Relations:**

$$\frac{T}{T_0} = \left(1 + \frac{\gamma - 1}{2} Ma^2\right)^{-1} \quad \texttt{[adiab, perf]} \quad (2.6)$$

$$\frac{p}{p_0} = \left(1 + \frac{\gamma - 1}{2} Ma^2\right)^{-\frac{\gamma}{\gamma-1}} \quad \texttt{[isen, perf]} \quad (2.7)$$

$$\frac{\rho}{\rho_0} = \left(1 + \frac{\gamma - 1}{2} Ma^2\right)^{-\frac{1}{\gamma-1}} \quad \texttt{[isen, perf]} \quad (2.8)$$

- **Critical Ratios:**

$$\frac{T_0}{T^*} = \frac{\gamma + 1}{2} \qquad \frac{\rho_0}{\rho^*} = \left(\frac{\gamma + 1}{2}\right)^{\frac{1}{\gamma-1}} \qquad \frac{p_0}{p^*} = \left(\frac{\gamma + 1}{2}\right)^{\frac{\gamma}{\gamma-1}} \quad (2.9)$$

Dimensionless Numbers & Viscosity

- **Reynolds Number:**

$$\mathrm{Re} = \frac{\rho V L}{\mu} = \frac{V L}{\nu} \quad (2.2)$$

- **Knudsen Number:**

$$\mathrm{Kn} = \frac{\lambda}{L_c} \quad (2.3)$$

- **Relation between major dimensionless numbers**

$$Kn = \frac{Ma}{Re} \sqrt{\frac{\gamma \pi}{2}} \quad (2.11)$$

- **Sutherland's Formula (Dynamic Viscosity):**

$$\mu(T) = \mu_0 \left(\frac{T}{T_0}\right)^{3/2} \frac{T_0 + S}{T + S} \quad (3.1)$$

Mass Flow Rate (Compressible, Isentropic Flow)

$$\dot{m} = A\, p_0 \sqrt{\frac{\gamma}{R T_0}}\, M \left(1 + \frac{\gamma - 1}{2} M^2\right)^{-\frac{\gamma+1}{2(\gamma-1)}} \quad (2.10)$$

Additional Useful Relations

- **Prandtl-Meyer Function (Expansion Fan):**

$$\nu(M) = \sqrt{\frac{\gamma + 1}{\gamma - 1}} \arctan\left(\sqrt{\frac{\gamma - 1}{\gamma + 1}(M^2 - 1)}\right) - \arctan\left(\sqrt{M^2 - 1}\right)$$

  The maximum turning angle is given by:

$$\theta_{\max} = \nu(M \to \infty) - \nu(M) \quad (3.10)$$

List of Figures

List of Tables

References

1. LAGIN, A. *Advancing Single-Atom Catalysis: Development of an Apparatus for Reactions at Near Ambient Pressure* [Poster presented at the Institute of Applied Physics, Vienna University of Technology (TU Wien), Surface Physics Group]. 2025. Project presentation.
2. LEISHMAN, J. Gordon. Internal Flows [online]. 2023 [visited on 2024-07-25]. Available from DOI: 10.15394/eaglepub.2022.1066.n26. Book Title: Introduction to Aerospace Flight Vehicles Publisher: Embry-Riddle Aeronautical University.
3. ÇENGEL, Yunus A.; CIMBALA, John M. *Fluid Mechanics: Fundamentals and Applications*. 4th. New York, NY: McGraw Hill, LLC, 2017. Mechanical Engineering.
4. ANDERSON, John D. *Modern Compressible Flow: With Historical Perspective*. 4th. New York: McGraw-Hill Education, 2021. ISBN 9781260570556.
5. RAPP, Bastian E. *Microfluidics: Modeling, Mechanics and Mathematics*. Oxford, UK: Elsevier, 2017. ISBN 978-1-4557-3141-1. Available from DOI: 10.1016/C2012-0-02230-2.
6. PUTIGNANO, Massimiliano. *Supersonic Gas-Jet Based Beam Profile Monitor*. Liverpool, UK, 2012. PhilosophiæDoctor (PhD). University of Liverpool.
7. HALWIDL, Daniel. *Development of an Effusive Molecular Beam Apparatus* [online]. Wiesbaden, 2016 [visited on 2023-09-28]. Available from DOI: 10.1007/978-3-658-13536-2. PhD thesis. Springer Fachmedien Wiesbaden.
8. CANTWELL, Brian. *AA210A: Fundamentals of Compressible Flow - Course Introduction*. 2020. Presentation slide with a rocket test image on cover.
9. BENSON, Ben. *Mass Flow Rate Equations* [online]. [N.d.]. [visited on 2025-01-27]. Available from: https://www.grc.nasa.gov/www/k-12/VirtualAero/BottleRocket/airplane/mchkdrv.html.
10. LI, Wen-Hsiung; LAM, Sau-Hai. *Principles of Fluid Mechanics*. Reading, Massachusetts: Addison-Wesley, 1964. Addison-Wesley Series in Engineering Science: Mechanics and Thermodynamics. Consulting editors: Bernard Budiansky and Howard W. Emmons.
11. *Fundamentals of Gas Dynamics* [online]. Princeton University Press, 1958 [visited on 2025-01-21]. ISBN 9780691626499. Available from: http://www.jstor.org/stable/j.ctt183pg9x.
12. JOUSTEN, Karl (ed.). *Handbook of vacuum technology*. Second, completely revised and updated edition. Weinheim: Wiley-VCH Verlag GmbH & Co. KGaA, 2016. ISBN 978-3-527-41338-6 978-3-527-68824-1 978-3-527-68823-4 978-3-527-68826-5 978-3-527-68825-8.
13. HIRSCHFELDER, J. O.; CURTISS, Charles F. .; BIRD, R. Byron. Molecular Theory Of Gases And Liquids. In: 1954. Available also from: https://api.semanticscholar.org/CorpusID:93258869.
14. KIM, Youn J.; KIM, You-Jae; HAN, J. -G. *Numerical analysis of flow characteristics of an atmospheric plasma torch*. 2004. Available from arXiv: physics/0410237 [physics.class-ph].
15. BIRD, G. A. *DSMC - The DSMC method*. Version 1.2. S.l.: G. A. Bird, 2013. ISBN 978-1-4921-1290-7.

16. GRABE, Martin. Numerical Simulation of Nitrogen Nozzle Expansion Using Kinetic and Continuum Approaches. In: *Proceedings of the 59th International Astronautical Conference 2008*. Glasgow, 2008. Open Access. Available at `https://elib.dlr.de/55152/`.

17. AMES RESEARCH STAFF. *Equations, Tables, and Charts for Compressible Flow*. Moffett Field, CA, 1953. Tech. rep., Report 1135. National Advisory Committee for Aeronautics. Available also from: `https://ntrs.nasa.gov/api/citations/19930091059/downloads/19930091059.pdf`.

18. COMSOL. *Microfluidics Module User's Guide*. Stockholm, Sweden: COMSOL AB, 2022. Version: COMSOL 6.1, Part number: CM021901. Available at: `www.comsol.com`.

19. SALAS, M.D.; ABARBANEL, S.; GOTTLIEB, D. Multiple steady states for characteristic initial value problems. *Applied Numerical Mathematics*. 1986, vol. 2, no. 3, pp. 193–210. ISSN 0168-9274. Available from DOI: `https://doi.org/10.1016/0168-9274(86)90028-0`. Special Issue in Honor of Milt Rose's Sixtieth Birthday.

20. AGRAWAL, Amit. A Comprehensive Review on Gas Flow in Microchannels. *International Journal of Micro-Nano Scale Transport* [online]. 2011, vol. 2, no. 1, pp. 1–40 [visited on 2024-07-09]. ISSN 1759-3093. Available from: `http://doi.org/10.1260/1759-3093.2.1.1`. Number: 1 Publisher: Multi-Science Publishing.

21. WANG, Moran; LAN, Xudong; LI, Zhixin. Analyses of gas flows in micro- and nanochannels. *International Journal of Heat and Mass Transfer* [online]. 2008, vol. 51, no. 13-14, pp. 3630–3641 [visited on 2024-11-18]. ISSN 00179310. Available from DOI: `10.1016/j.ijheatmasstransfer.2007.10.011`.

22. KHARE, Shivang; SAHA, Ujjwal K. Rocket nozzles: 75 years of research and development. *Sādhanā* [online]. 2021, vol. 46, no. 2, p. 76 [visited on 2024-08-21]. ISSN 0973-7677. Available from DOI: `10.1007/s12046-021-01584-6`.

23. FERNANDES, Tiago; SOUZA, Alain; AFONSO, Frederico. A shape design optimization methodology based on the method of characteristics for rocket nozzles. *CEAS Space Journal* [online]. 2023, vol. 15, no. 6, pp. 867–879 [visited on 2024-08-21]. ISSN 1868-2510. Available from DOI: `10.1007/s12567-023-00511-1`.

24. CASSANOVA, R. A.; STEPHENSON, W. B. *Expansion of a Jet into Near Vacuum*. 1965-08. Tech. rep., AEDC-TR-65-151. Aerospace Environmental Facility, Arnold Engineering Development Center, Air Force Systems Command, Arnold Air Force Station, Tennessee. Available also from: `https://apps.dtic.mil/sti/tr/pdf/AD0469041.pdf`. Approved for public release; distribution is unlimited.

25. ROBERTSON, S. J. *Investigation of the steady expansion of a gaseous axisymmetric jet into a vacuum Final report* [online]. 1970-01. [visited on 2024-08-22]. Tech. rep., HREC-1490-2. Available from: `https://ntrs.nasa.gov/citations/19700021503`. NTRS Author Affiliations: Lockheed Missiles and Space Co. NTRS Document ID: 19700021503 NTRS Research Center: Legacy CDMS (CDMS).

26. *Zucrow, Hoffman - Gas Dynamics, Vol. 2 - 1977.pdf* [online]. [N.d.]. [visited on 2024-08-22]. Available from: `http://ftp.demec.ufpr.br/CFD/bibliografia/Zucrow,%20%20Hoffman%20-%20Gas%20Dynamics,%20Vol.%202%20-%201977.pdf`.

27. ANDERSON, John D. *Fundamentals of aerodynamics*. Sixth edition. New York, NY: McGraw Hill Education, 2017. McGraw-Hill series in aeronautical and aerospace engineering. ISBN 978-1-259-12991-9.

28. LIU, Minghou; ZHANG, Xianfeng; ZHANG, Genxuan; CHEN, Yiliang. Study on micronozzle flow and propulsion performance using DSMC and continuum methods. *Acta Mechanica Sinica* [online]. 2006, vol. 22, no. 5, pp. 409–416 [visited on 2025-02-24]. ISSN 1614-3116. Available from DOI: 10.1007/s10409-006-0020-y.

A Calculations

A.1 Algebraic Calculations - SMath

See: `https://smath.com/` for an online smath editor

Variable Definitions:

$\gamma := 1.47 \quad M_m := 28.01 \frac{gram}{mol} \quad R_s := \frac{R_m}{M_m} = 296.8394 \cdot \frac{1}{K} \frac{J}{kg}$

$A_3 := 100000 \, micron^2 = 0.1 \, mm^2 \quad A_4 := 100 \cdot \pi \, micron^2 \quad A_5 := 400 \cdot \pi \, micron^2$

$T_t := 500 \, K \quad p_t := 1.5 \, bar \quad A_2 := A_4 \quad A_1 := A_5$

$L_{c.1} := 40 \, micron \quad L_{c.2} := 40 \, micron \quad L_{c.3} := 40 \, micron \quad L_{c.4} := 20 \, micron \quad L_{c.5} := 40 \, micron$

Function Definitions:

Isentropic Massflow:

$massflow(\gamma, M, A, T_t, p_t) := A \cdot p_t \cdot \sqrt{\frac{\gamma}{R_s \cdot T_t}} \cdot M \cdot \left(1 + \frac{\gamma - 1}{2} \cdot M^2\right)^{-\frac{\gamma + 1}{2 \cdot (\gamma - 1)}}$

Dynamic Viscosity using sutherlands formular:

$\mu_{ref} := 1.716 \cdot 10^{-5} \frac{N \, s}{m^2} \quad T_{ref} := 276 \, K \quad S_\mu := 111 \, K$

$sutherland(T) := \mu_{ref} \cdot \left(\frac{T}{T_{ref}}\right)^{\frac{3}{2}} \cdot \frac{T_{ref} + S_\mu}{T + S_\mu}$

$p_{crit.ratio} := \left(\frac{2}{\gamma + 1}\right)^{\frac{\gamma}{\gamma - 1}} = 0.5168$

$T_{crit.ratio} := \frac{2}{\gamma + 1} = 0.8097$

Knudsen number:

$knudsen(p, T, L_c) := \frac{sutherland(T) \cdot R_s}{p \cdot L_c} \cdot \sqrt{\frac{\pi \cdot M_m \cdot T}{2 \, k \, N_A}}$

Reynolds number:

$reynolds(p, T, L_c, Ma, \gamma) := \frac{knudsen(p, T, L_c)}{Ma} \cdot \sqrt{\frac{2}{\gamma \cdot \pi}}$

Isentropic Relations:

$temp\_to\_total(\gamma, M) := \left(1 + \frac{\gamma - 1}{2} \cdot M^2\right)^{-1} \quad pressure\_to\_total(\gamma, M) := \left(1 + \frac{\gamma - 1}{2} \cdot M^2\right)^{-\frac{\gamma}{\gamma - 1}}$

$density\_to\_total(\gamma, M) := \left(1 + \frac{\gamma - 1}{2} \cdot M^2\right)^{-\frac{1}{\gamma - 1}}$

Machnumber solvers:

$solve\_machnumber\_sub(A_{ratio}, \gamma) := solve\left(\frac{1}{M} \cdot \left(\left(\frac{2}{\gamma + 1}\right) \cdot \left(1 + \frac{\gamma - 1}{2} \cdot M^2\right)\right)^{\frac{\gamma + 1}{2 \cdot (\gamma - 1)}} - A_{ratio} = 0, M, 0, 1\right)$

$solve\_machnumber\_super(A_{ratio}, \gamma) := solve\left(\frac{1}{M} \cdot \left(\left(\frac{2}{\gamma + 1}\right) \cdot \left(1 + \frac{\gamma - 1}{2} \cdot M^2\right)\right)^{\frac{\gamma + 1}{2 \cdot (\gamma - 1)}} - A_{ratio} = 0, M, 1, 12\right)$

Chapter 3.3: one-dimensional isentropic case

Position 3 (middle of Reactor):

$M_{3.1} := solve\_machnumber\_sub(318, \gamma) =$

From external Solver:

$M_{3.1} := 0.0018$

$M_{3.2} := solve\_machnumber\_super(318, \gamma) = 10.543$

$m_{3.1} := massflow(\gamma, M_{3.1}, A_3, T_t, p_t) = 8.4972 \cdot 10^{-8} \frac{kg}{s}$

$m_{3.2} := massflow(\gamma, M_{3.2}, A_3, T_t, p_t) = 8.5253 \cdot 10^{-8} \frac{kg}{s}$

$p_{3.1.to.total} := pressure\_to\_total(\gamma, M_{3.1}) = 1$
$T_{3.1.to.total} := temp\_to\_total(\gamma, M_{3.1}) = 1$

$p_{3.2.to.total} := pressure\_to\_total(\gamma, M_{3.2}) = 3.2891 \cdot 10^{-5}$
$T_{3.2.to.total} := temp\_to\_total(\gamma, M_{3.2}) = 0.0369$

Position 2 & 4 (nozzle throats):

$m_{2.4} := massflow(\gamma, 1, A_4, T_t, p_t) = 8.517 \cdot 10^{-8} \frac{kg}{s}$

$p_{2.4.to.total} := pressure\_to\_total(\gamma, 1) = 0.5168$

$\rho_{2.4.to.total} := density\_to\_total(\gamma, 1) = 0.6382$

$T_{2.4.to.total} := temp\_to\_total(\gamma, 1) = 0.8097$

Position 5 (outlet nozzle exit plane):

$M_{5.1} := solve\_machnumber\_sub(4, \gamma) = 0.1455$
$m_{5.1} := massflow(\gamma, M_{5.1}, A_5, T_t, p_t) = 8.5169 \cdot 10^{-8} \frac{kg}{s}$

$p_{5.1.to.total} := pressure\_to\_total(\gamma, M_{5.1}) = 0.9846$

$\rho_{5.1.to.total} := density\_to\_total(\gamma, M_{5.1}) = 0.9895$

$T_{5.1.to.total} := temp\_to\_total(\gamma, M_{5.1}) = 0.9951$

$M_{5.2} := solve\_machnumber\_super(4, \gamma) = 3.063$
$m_{5.2} := massflow(\gamma, M_{5.2}, A_5, T_t, p_t) = 8.517 \cdot 10^{-8} \frac{kg}{s}$

$p_{5.2.to.total} := pressure\_to\_total(\gamma, M_{5.2}) = 0.0262$

$\rho_{5.2.to.total} := density\_to\_total(\gamma, M_{5.2}) = 0.0839$

$T_{5.2.to.total} := temp\_to\_total(\gamma, M_{5.2}) = 0.312$

Chapter 3.3: one-dimensional isentropic knudsen and reynolds numbers

knudsen numbers:

$Kn_1 := knudsen(p_t, T_t, L_{c.1}) = 0.0021$
$Kn_{2.4} := knudsen(p_t \cdot p_{2.4.to.total}, T_t \cdot T_{2.4.to.total}, L_{c.2}) = 0.0032$

$Kn_{3.1} := knudsen(p_t \cdot p_{3.1.to.total}, T_t \cdot T_{3.1.to.total}, L_{c.3}) = 0.0021$
$Kn_{3.2} := knudsen(p_t \cdot p_{3.2.to.total}, T_t \cdot T_{3.2.to.total}, L_{c.3}) = 0.4161$

$Kn_{5.1} := knudsen(p_t \cdot p_{5.1.to.total}, T_t \cdot T_{5.1.to.total}, L_{c.5}) = 0.0022$
$Kn_{5.2} := knudsen(p_t \cdot p_{5.2.to.total}, T_t \cdot T_{5.2.to.total}, L_{c.5}) = 0.0181$

reynolds numbers:

$Re_1 := reynolds(p_t, T_t, L_{c.1}, 0.001, \gamma) = 1.4035$
$Re_{2.4} := reynolds(p_t, T_t, L_{c.2}, 1, \gamma) = 0.0014$

$Re_{3.1} := reynolds(p_t, T_t, L_{c.3}, M_{3.1}, \gamma) = 0.7797$
$Re_{3.2} := reynolds(p_t, T_t, L_{c.3}, M_{3.2}, \gamma) = 0.0001$

$Re_{5.1} := reynolds(p_t, T_t, L_{c.5}, M_{5.1}, \gamma) = 0.0096$
$Re_{5.1} := reynolds(p_t, T_t, L_{c.5}, M_{5.2}, \gamma) = 0.0005$

Chapter 3.5: Disconneted Reservoirs (Isentropic):

$M_{D.iso} := \left(1 + \frac{\gamma - 1}{2}\right)^{-\frac{\gamma + 1}{2 \cdot (\gamma - 1)}} = 0.5743$

$p_{ratio} := pressure\_to\_total(\gamma, M_{D.iso}) = 0.7918$
$T_{ratio} := temp\_to\_total(\gamma, M_{D.iso}) = 0.9281$

$\rho_{ratio} := density\_to\_total(\gamma, M_{D.iso}) = 0.8531$

$m_{D.term} := massflow(\gamma, M_{D.iso}, A_2, T_t, p_t) = 7 \cdot 10^{-8} \frac{kg}{s}$

Chapter 3.5: Disconneted Reservoirs (Isothermal):

$$f := \left(-\frac{1}{\gamma - 1} + \sqrt{\frac{1}{(\gamma - 1)^2} + \frac{2}{\gamma - 1} \cdot \left(\frac{2}{\gamma + 1} \right)^{\frac{\gamma + 1}{\gamma - 1}}} \right) = 0.3076 \qquad M_{D.term} := \sqrt{f} = 0.5546$$

$$p_{ratio} := pressure\_to\_total\left(\gamma, M_{D.term}\right) = 0.8039 \qquad T_{ratio} := temp\_to\_total\left(\gamma, M_{D.term}\right) = 0.9326$$

$$\rho_{ratio} := density\_to\_total\left(\gamma, M_{D.term}\right) = 0.862$$

$$m_{D.term} := massflow\left(\gamma, M_{D.term}, A_2, T_t, p_t\right) = 6.8468 \cdot 10^{-8}\ \frac{kg}{s}$$

Chapter 3.5: Formulation with leak (isentopic connection):

$$m_{L.isen}\left(A, \gamma, T_r, p_r\right) := A \cdot p_r \cdot \sqrt{\frac{\gamma}{R_s \cdot T_r}} \cdot \left(1 - \left(1 + \frac{\gamma - 1}{2} \right)^{-\frac{\gamma + 1}{2 \cdot (\gamma - 1)}} \right)$$

$$p_r := p_{crit.ratio} \cdot p_t = 0.7752\ bar \qquad T_r := T_{crit.ratio} \cdot T_t = 404.8583\ K$$

$$m_{L.isen}\left(A_4, \gamma, T_r, p_r\right) = 3.6258 \cdot 10^{-8}\ \frac{kg}{s}$$

Chapter 3.5: Formulation with leak (isothermal connection):

$$m_{L.iso}\left(A, \gamma, T, p_r\right) := A \cdot p_r \cdot \sqrt{\frac{\gamma}{R_s \cdot T}} \cdot \left(1 + \frac{\gamma - 1}{2} \right)^{-\frac{\gamma + 1}{2 \cdot (\gamma - 1)}} \cdot \left(\left(1 + \frac{\gamma - 1}{2} \right)^{\frac{\gamma}{\gamma - 1}} - 1 \right)$$

$$m_{L.iso}\left(A_4, \gamma, T_r, p_r\right) = 4.5737 \cdot 10^{-8}\ \frac{kg}{s}$$

Chapter 3.2: expected knudsen number

Test:

$$\alpha := 0.06\ \frac{Pa}{K^{\frac{3}{2}}} \qquad Kn := knudsen\left(1\ bar, 300\ K, 20\ micron\right) = 0.0034$$

$$p := \alpha \cdot \frac{T_t^{\frac{3}{2}}}{0.1} = 0.0671\ bar \qquad p := 1\ bar$$

$$a := \frac{p \cdot Kn}{T_t^{\frac{3}{2}}} = 0.0021\ \frac{Pa}{K^{\frac{3}{2}}}$$

Chapter 3.6: Maximum turning angle

$$\theta_{max} := \frac{\pi}{2} \cdot \left(\sqrt{\frac{\gamma + 1}{\gamma - 1}} - 1 \right) - \sqrt{\frac{\gamma + 1}{\gamma - 1}} \cdot atan\left(\sqrt{\frac{\gamma - 1}{\gamma + 1} \cdot \left(M_{5.2}^2 - 1 \right)} \right) + atan\left(\sqrt{M_{5.2}^2 - 1} \right) = 68.912\ deg$$

A.2 Python

Packages:

- NumPy: `https://numpy.org/`
- SciPy: `https://scipy.org/`

A.2.1 Sutherland minimum mean square error

Listing 1: Minimum mean square error best fit linearization for Sutherland formula

```
import numpy as np

def sutherland(T, mu_ref=1.716e-5, T_ref=273.15, S=110.4):
    return mu_ref * (T / T_ref) ** (3/2) * (T_ref + S) / (T + S)

# Generate temperatures and compute dynamic viscosities
T_values = np.linspace(200, 1000, 100)
mu_values = sutherland(T_values)

# Filter data for the range between 200 and 600 K
mask = (T_values >= 200) & (T_values <= 600)
T_fit = T_values[mask]
mu_fit = mu_values[mask]

# Compute the best-fit linear regression over the selected range
slope, intercept = np.polyfit(T_fit, mu_fit, 1)
print(f"Slope: {slope}, Intercept: {intercept}")

slope_i0 = np.sum(T_fit * mu_fit) / np.sum(T_fit**2)
print(f"Slope: {slope_i0} with intercept = 0")
```

A.2.2 Solve Mach number from area ratio

Listing 2: Solve Mach number from area ratio using scipy fsolve from: code/solve-mach-number.py)

```
import numpy as np
from scipy.optimize import fsolve

def mach_area_relation(M, A_Astar, gamma):
    """Equation to solve for Mach number M."""
    return (1 / M) * ((2 / (gamma + 1)) * (1 + ((gamma - 1) / 2) * M**2))
        **((gamma + 1) / (2 * (gamma - 1))) - A_Astar

def solve_mach(A_Astar, gamma, M_guess=1.0):
    """Solves for Mach number M given A/A* and gamma."""
    M_solution = fsolve(mach_area_relation, M_guess, args=(A_Astar, gamma
        ))
    return M_solution[0]

A_Astar = 318
gamma = 1.47
M_solution = solve_mach(A_Astar, gamma, 0.1)
print(f"Solved Mach number: {M_solution:.5f}")
```